https://doi.org/10.5194/egusphere-2023-1597
Preprint. Discussion started: 22 September 2023

Evaluation of root-zone soil moisture products over the Huai river basin

En Liu[1,2], Yonghua Zhu[1], Jean-christophe Calvet[2], Haishen Lü[1], Bertrand Bonan[2], Jingyao Zheng[1], Qiqi Gou[1], Xiaoyi Wang[1], Zhenzhou Ding[1], Haiting Xu[1], Ying Pan[1], Tingxing Chen[1]

[1]State Key Laboratory of Hydrology-Water Resources and Hydraulic Engineering, 14 College of Hydrology and Water Resources, Hohai University, Nanjing 210098, China
[2]CNRM, Université de Toulouse, Météo-France, CNRS, 31057, Toulouse, France

Correspondence to: Yonghua Zhu (zhuyonghua@hhu.edu.cn)

Abstract: Root zone soil moisture (RZSM) is critical for water resource management, drought monitoring and sub-seasonal flood climate prediction. RZSM is not directly observable from space, but several RZSM products are available and widely used at global and continental scales. This paper presents a comprehensive quantitative evaluation of eight RZSM products over the Huai River Basin (HRB) in China. A direct validation is performed using observations from 58 *in situ* soil moisture stations from 1 April 2015 to 31 March 2020. Attention is drawn to the potential factors that increase the uncertainties of model-based RZSM, such as errors in atmospheric forcing (precipitation, air temperature), soil properties, and spatial scale mismatch. The results show that the Global Land Data Assimilation System Catchment Land Surface Model (GLDAS_CLSM) performs best among all RZSM products with the highest correlation coefficient (*R*) and the lowest unbiased root mean square error (ubRMSE): 0.69 and 0.018 $m^3 m^{-3}$, respectively. All RZSM products tend to overestimate *in situ* soil moisture values, except for the Soil Moisture and Ocean Salinity (SMOS) L4 product, which underestimates RZSM. The underestimation of Surface Soil Moisture (SSM) in SMOS L3, caused by underestimated physical surface temperature and overestimated ERA interim soil moisture, triggers the underestimation of RZSM in SMOS L4. The overestimation of RZSM by the other products can be explained by the overestimation of precipitation, the frequency of precipitation events (drizzle effects) and the underestimation of air temperature. In addition, the overestimation of soil clay content and the underestimation of soil sand content in different LSMs lead to higher soil moisture values. The intercomparison of the eight RZSM products shows that MERRA-2 and SMAP L4 RZSM have the highest correlation, which can be attributed to the fact that both products use the catchment land surface model and the atmospheric forcing provided by the Goddard Earth Observing System Model, version 5 (GEOS-5), although the versions differ slightly.

https://doi.org/10.5194/egusphere-2023-1597
Preprint. Discussion started: 22 September 2023

1 Introduction

Soil moisture plays a key role in the hydrological cycle and land-atmosphere interactions. It controls water and energy balances (Calvet, 2000; Brocca et al., 2010; Xing et al., 2021) and has been recognised by the World Meteorological Organization (WMO) as one of the 50 essential climate variables (Cho et al., 2015). In particular, root zone soil moisture (RZSM) has important applications in agricultural drought monitoring, water resource management, flood forecasting and seasonal climate prediction (Reichle et al., 2017a; Zhou et al., 2020; Beck et al., 2021; Xing et al., 2021; Xu et al., 2021; Fan et al., 2022). RZSM is the amount of water held in the soil that is available for plant transpiration and biomass production, which is crucial for agricultural drought monitoring. Different ecosystems in different climate and topography conditions have different rooting depth, and root zone water storage capacity (Gao et al., 2014; Kleidon, 2014; Fan et al., 2017; Gao et al., 2019). For example, trees in arid regions must have deep rooting depth and large root zone water storage capacity, otherwise they cannot survive in drought (Yang et al., 2016). Crops usually have shallower rooting and in agricultural applications, RZSM is commonly defined as the volumetric soil moisture in the top 1 m of the soil column (Reichle et al., 2015; Babaeian et al., 2019; Al Bitar et al., 2021; Huerta-Bátiz et al., 2022). This definition of RZSM has been widely used in many existing studies (Reichle et al., 2017a; Pablos et al., 2018; Xing et al., 2021; Xu et al., 2021; Fan et al., 2022). In the context of climate change, extreme events such as floods, droughts and heat waves are becoming more frequent around the world, with significant impacts on RZSM (Lorenz et al., 2010; Hauser et al., 2016; Al Bitar et al., 2021). For example, flash droughts are severely affecting RZSM and agricultural production in the Huaibei Plain, China (Gou et al., 2022).

Recent satellite soil moisture missions provide global surface soil moisture (SSM) retrievals with approximately 3-day temporal resolution, but are limited to the top few centimetres (0-5 cm for L-band) due to microwave penetration depth limitations (Kerr et al., 2001; Reichle et al., 2017b). As a result, several RZSM products have been developed for broader global applications. For example, RZSM products such as the Global Land Data Assimilation System (GLDAS) (Rodell et al., 2004), the China Land Data Assimilation System (CLDAS) (Shi et al., 2014) and the Soil Moisture Active Passive (SMAP) Level 4 (L4) (Reichle et al., 2012; Reichle et al., 2017a) have been developed. These products aim to provide optimal land surface states and fluxes by combining an offline (not coupled to the atmosphere) land surface model (LSM) with satellite data using data assimilation techniques (Calvet and Noilhan, 2000; Rodell et al., 2004). The LSM is forced with meteorological analysis fields including precipitation, wind speed, air humidity, surface pressure, air temperature and radiation. The European Centre for Medium-Range Weather Forecasts (ECMWF) fifth generation reanalysis (ERA5) (Hersbach et al., 2020), the Modern-Era Retrospective Analysis for Research and Applications version 2 (MERRA-2) (Gelaro et al., 2017), and the National Centers for Environmental Prediction Climate Forecast System version 2 (NCEP CFSv2) (Saha et al., 2014) provide global analysis of atmospheric fields. They also provide sub-daily ocean and land surface variables. These fields are generated by coupling an Atmospheric General Circulation Model (AGCM) with an LSM and an Ocean Wave Model (OWM), and by assimilating a large number of *in situ* and satellite observations. In addition, the Soil Moisture and Ocean Salinity (SMOS) Centre Aval de Traitement des Données (CATDS) provides SMOS L4 RZSM products, which are derived from SMOS Level 3 (L3) 3-day SSM retrievals using a statistical exponential filter model (Albergel et al., 2008; Al Bitar and Mahmoodi, 2020).

Numerous studies have been conducted to validate and assess the utility of SSM using *in situ* observations in the topsoil layer (Collow et al., 2012; Cui et al., 2017; Beck et al., 2021; Zheng et al., 2022). On the other hand,

https://doi.org/10.5194/egusphere-2023-1597
Preprint. Discussion started: 22 September 2023

validation studies for RZSM are relatively rare, especially over China (Xing et al., 2021; Xu et al., 2021; Fan et al., 2022). Given the importance of the Huai River Basin (HRB) as an agricultural grain production area in China, it is crucial to evaluate the performance of different RZSM products in this region. RZSM products can be validated against *in situ* observations, which serve as a reference dataset. Differences between *in situ* RZSM observations and RZSM products can be attributed to errors in meteorological forcing data, soil properties, parameterisation and scale mismatch, etc.

The accuracy of RZSM products is strongly influenced by the quality of meteorological forcing data, especially precipitation and air temperature (Zeng et al., 2021). Numerous studies have shown large uncertainties in global climate atmospheric forcing data, particularly for precipitation frequency, intensity and heavy precipitation events (Sun et al., 2005; Piani et al., 2010; Velasquez et al., 2020; Jiao et al., 2021). Accurate representation of soil properties is also critical. Many global LSMs rely on the FAO/UNESCO (Food and Agriculture Organization, United Nations Educational, Scientific and Cultural Organization) World Soil Map (Reynolds et al., 2000), including GLDAS products (Bi et al., 2016; Yang et al., 2020), NCEP CFSv2 (Yang et al., 2020), ERA5 (Qin et al., 2017; Yang et al., 2020), SMOS L4 (Al Bitar et al., 2021), MERRA-2 (McCarty et al., 2016; Gelaro et al., 2017). However, this soil map contains limited soil information in many regions, including China (Shangguan et al., 2013), leading to increased uncertainty in soil moisture simulations. In addition, the lack of representation of soil stratification can significantly affect the simulation of RZSM by LSMs. In the Huaibei Plain, the stratification of plough, black soil and lime concretion layers can hinder the vertical movement of water from the surface layer to the root zone layer (Li et al., 2011; Zha et al., 2015; Gu et al., 2021). Finally, the accuracy of soil moisture simulations is also affected by different model structures and parameterisations. Different LSMs are used in LDAS or reanalysis products, such as the Noah LSM in GLDAS_NOAH and NCEP CFSv2 (Rodell et al., 2004; Saha et al., 2014), HTESSEL in ERA5 (Hersbach et al., 2020), CLSM in GLDAS_CLSM, MERRA-2 and SMAP L4 (Koster et al., 2000; Reichle et al., 2017c; Reichle et al., 2021), the Common Land Model (CoLM) and the Community Noah LSM with multi-parameterisation options (Noah-MP) in CLDAS products (Wang et al., 2021a). The exponential filter technique is used in SMOS L4 (Al Bitar et al., 2021).

The objectives of this study are to (1) compare eight global RZSM products (ERA5, MERRA-2, NCEP CFSv2, GLDAS_CLSM v2.2, GLDAS_NOAH v2.1, CLDAS v2. 0, SMAP L4 and SMOS L4) with *in situ* soil moisture observations over the HRB from 1 April 2015 to 31 March 2020, (2) compare the RZSM products with each other over the HRB, (3) investigate the potential sources of errors on the performance of the RZSM products, including meteorological forcing data, soil properties and soil stratification. As it is difficult to directly quantify the effects of model structures and parameterisations on soil moisture, these aspects are not addressed in this study. The paper is organized as follows. The gridded RZSM products and *in situ* validation datasets (precipitation, air temperature, soil texture) are presented in Sect. 2. Section 3 describes the RZSM pre-processing methods and the statistical metrics used to evaluate the different datasets. The validation and the intercomparison of the RZSM products are presented in Sect. 4. Section 5 discusses the potential sources of error in various RZSM products. Section 6 provides the main conclusions.

https://doi.org/10.5194/egusphere-2023-1597
Preprint. Discussion started: 22 September 2023

2 Datasets

In this study, RZSM is defined as the volumetric soil moisture in the top 1 m of the soil column. The eight RZSM products evaluated in this study are summarised in Table 1.

2.1 The HRB study area

The HRB is the transitional zone between the northern subtropical and warm temperate climates, and it is one of the most important commodity grain production areas in China. It is located in eastern China, 111°55′-121°25′ E, 30°55′-36°36′N, and covers an area of 270000 km^2 (Figure 1). The HRB has a typical humid and sub-humid monsoon climate. The average annual precipitation is 888 mm and increases from north to south. More than 60 % of the annual precipitation falls between June and September (Zhang et al., 2009). The HRB suffers from frequent floods and droughts due to the spatial and temporal variability of precipitation and evaporation. The main land cover types in the HRB are rainfed croplands, followed by irrigated croplands, forests and grasslands. Overall, the terrain of the HRB is relatively flat, with a large plain covering 90 % of the area. The cultivated area in the HRB is approximately 127200 km^2, of which 76 % is irrigated according to the Manual of the Huai River Basin Irrigation Area (Chapter 2.1) and Summary of Flood Control Planning for the Huai River Basin (http://www.hrc.gov.cn). The water resource infrastructures include reservoirs, electromechanical wells, diversion locks and pumping stations built along lakes and rivers. Most cropland fields are irrigated by irrigation canals or a combination of wells and canals (Wang et al., 2021a). Annual evaporation can exceed precipitation. It ranges from 900 to 1500 mm and decreases from north to south (Wang et al., 2021a). Heavy irrigation in the HRB can explain the extra water available for evaporation.

2.2 HRB *in situ* measurements

The HRB soil moisture network was established by the Ministry of Water Resources of the People's Republic of China. It consists of 58 *in situ* stations (see Table S1) and provides soil moisture measurements at four depths of 10, 20, 40 and 100 cm (Liu et al., 2023). At each station, volumetric soil moisture measurements in units of m^3 m^{-3} are collected at 08:00 AM local solar time using frequency domain reflectometry ECH$_2$O EC-TM probes. These probes are calibrated using gravimetric measurements taken at each soil depth. The deployment of the soil moisture stations and the collection of soil moisture measurements follows the specifications for soil moisture monitoring (MWR, 2015). Since the study aims to evaluate the accuracy of RZSM products (0-100 cm), the soil moisture measurements at the four depths are depth-weighted averaged to obtain the 0-100 cm soil moisture data. Stations are located in areas without irrigation.

The China Daily Gridded Ground Precipitation and Air Temperature dataset V2.0, provided by the China Meteorological Administration (CMA) (http://data.cma.cn) with a spatial resolution of 0.5°×0.5°, serves as a reference dataset for validating the meteorological forcing fields used in reanalyses and LDAS. The CMA dataset is derived by spatial interpolation using the partial thin-plate smoothing spline method from 2474 ground-based meteorological station observations across China, following stringent quality controls and necessary corrections. At the national level, the average coverage of gauging stations in a grid cell is 38 %. However, in the eastern part of China, where the HRB is located, the coverage reaches up to 77 %. The dataset has been extensively validated and is of high quality. For example, the precipitation data has a root mean square error (RMSE) of 0.49 mm/month and a correlation coefficient (R) of 0.93 with a significance level p smaller than 0.01 (CMA, 2012b). The annual

https://doi.org/10.5194/egusphere-2023-1597
Preprint. Discussion started: 22 September 2023

145 air temperature data have a mean bias and RMSE ranging from -0.2 to 0.2°C and from 0.2 to 0.3°C, respectively (CMA, 2012a).

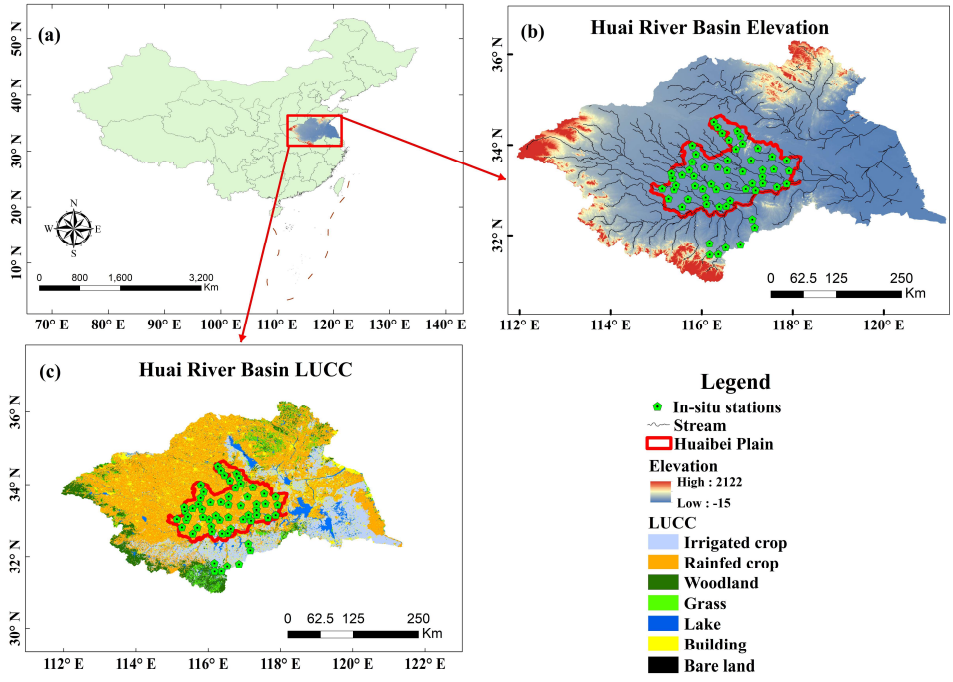

Fig. 1 Overview of the study area and distribution and land cover of *in situ* soil moisture stations (green pentagon).

2.3 Soil map

150 Soil databases used in many global LSMs have traditionally relied on the FAO/UNESCO 1:5 million scale World Soil Map. It took twenty years to complete this map, which remained the primary global overview of soil resources until recently (Shangguan et al., 2013). However, this FAO/UNESCO soil map contained limited soil information in different regions, including China. Consequently, the uncertainties in soil properties contributed to larger errors in the variables simulated by LSMs (e.g. RZSM), especially over China (Nachtergaele et al., 2009; Shangguan et
155 al., 2013). To address these uncertainties, the Harmonised World Soil Database (HWSD) was developed by FAO and the International Institute for Applied Systems Analysis (IIASA) with a resolution of 30 arcseconds. The HWSD combines recently collected regional and national updates of soil information with the FAO/UNESCO 1:5 million scale World Soil Map (FAO et al., 2012). HWSD also incorporates the 1:1 million scale soil map of China provided by the Institute of Soil Science, Chinese Academy of Sciences (ISSCAS).

160 The soil dataset developed by Shangguan et al. (2013), which integrates the physical and chemical properties of 8979 soil profiles along with the soil map of China (Shangguan et al., 2013), is employed in the CLDAS (Qin et al., 2017). The dataset provides information on soil properties for eight layers (0-2.3 m) at a spatial resolution of 30×30 arcseconds. Due to the limited availability of measured soil data, the soil properties information, including sand and clay content, bulk density and soil organic matter, from Shangguan et al. (2013) was used in
165 this study to validate the accuracy of the corresponding data from the FAO/UNESCO soil map and HWSD.

https://doi.org/10.5194/egusphere-2023-1597
Preprint. Discussion started: 22 September 2023

2.4. Gridded RZSM products

The eight products considered in this study (Table 1) are presented below.

2.4.1 ERA5

ERA5 is the fifth generation global atmospheric reanalysis produced by ECMWF. It covers the period from January 1940 to present and provides hourly estimates of 0.25 degree atmosphere, land surface and 0.5 degree ocean waves (Hersbach et al., 2023). ERA5 is developed using the 4-Dimensional Variational (4D-Var) data assimilation method, which incorporates a 10-member ensemble and model forecasts from the ECMWF Integrated Forecast System (IFS) in CY41R2 with 137 hybrid sigma/pressure model levels in the vertical and the top level at 0.01 hPa (Hersbach et al., 2020). The 4D-Var data assimilation uses 12-hour windows from 0900 UTC to 2100 UTC and from 2100 UTC to 0900 UTC (next day). The HTESSEL scheme is used as the land surface component of ERA5 to model land surface variables. Different techniques are used to assimilate the different variables: the Simplified Extended Kalman Filter (SEKF) is used for RZSM, 1-dimensional Optimal Interpolation (OI) for soil and snow temperature, 2-dimensional OI for snow and screen level parameters (2 m temperature and relative humidity) (Hersbach et al., 2020). The screen-level parameters analysis is carried out first, then its increments are incorporated into the soil moisture analysis.

2.4.2 MERRA-2

MERRA-2 is the latest version of a global atmospheric reanalysis product produced by NASA Global Modelling and Assimilation Office (GMAO, 2015). It uses the Goddard Earth Observing System Model (GEOS-5.12.4) atmospheric data assimilation system, which consists of (1) the GEOS atmospheric model and (2) the Gridpoint Statistical Interpolation assimilation system. It covers the period from January 1980 to present with a latency of approximately 3 weeks after the end of a month and provides global, hourly, 0.25-degree estimates (GMAO, 2015; Reichle et al., 2017c). CLSM is used as the land surface component of MERRA-2 to analyse the land surface states and fluxes. The precipitation forcing is the weighted average of model background precipitation generated by GEOS-5 FP-IT (Forward Processing system for Instrument Teams) after 31 December 2014 and precipitation generated by AGCM, with weights dependent on latitude. The National Oceanic and Atmospheric Administration (NOAA) Climate Prediction Center (CPC) Unified Gauge-Based Analysis of Global Daily Precipitation (CPCU) product is used to correct the model background precipitation. The CPC Merged Analysis of Precipitation (CMAP) product is rescaled to match the climatology of the Global Precipitation Climatology Project product, version 2.1 (GPCPv2.1) and is fully used in Africa, which allows the observed precipitation to impact, via evapotranspiration, the near-surface air temperature and humidity, thereby yielding a more self-consistent near-surface meteorological dataset (Reichle et al., 2017c).

2.4.3 NCEP CFSv2

NCEP CFSv2 is a global, high-resolution, coupled atmosphere-ocean-land surface-sea ice system designed to provide the best estimate of the state of these coupled domains, covering the period from January 2011 to present and providing 6-hourly, 0.2-degree estimates (Saha and coauthors, 2011). The Noah land surface model is used in the semi-coupled Climate Forecast System Reanalysis (CFSR) Global Land Data Assimilation System (GLDAS) to provide the land surface analysis and evolving land surface states (Saha et al., 2010; Saha et al., 2014) .

https://doi.org/10.5194/egusphere-2023-1597
Preprint. Discussion started: 22 September 2023

2.4.4 GLDAS_NOAH

GLDAS_NOAH version 2.1 provides global, 3-hourly, 0.25-degree resolution of estimates for the period from 1 January 2000 to present (Rodell et al., 2004; Beaudoing et al., 2020). The offline (not coupled to the atmosphere) Noah LSM is forced with combination of model- (NOAA/Global Data Assimilation System (GDAS) atmospheric analysis fields) and observation-based precipitation (the disaggregated Global Precipitation Climatology Project (GPCP) V1.3 Daily Analysis precipitation fields) and radiation data (the Air Force Weather Agency's AGRicultural METeorological modeling system (AGRMET) radiation fields) to provide optimal fields of land surface analysis (Rui et al., 2021).

2.4.5 GLDAS_CLSM

GLDAS_CLSM version 2.2 is based on the CLSM forced with the meteorological analysis fields from the operational ECMWF IFS and provides global, daily, 0.25-degree resolution estimates for the period from 1 February 2003 to present (Li et al., 2019; Li et al., 2020). GLDAS-2.2 assimilates observations of the total terrestrial water (TWS) anomaly from Gravity Recovery and Climate Experiment (GRACE). Temporal changes of TWS are influenced by changes in soil moisture, snow and ice, surface water and biomass, and groundwater storage.

2.4.6 CLDAS

The CLDAS-2.0 product is developed and released by CMA based on a multi-LSMs operational system consisting of CLM, CoLM, and Noah-MP, with a spatial coverage of 0-60° N and 70-150° E and temporal coverage from January 2008 to present (CMA, 2015). The production of CLDAS-V2.0 involves the following three processes. Firstly, nearly 40000 automated meteorological station measurements, ECMWF and NCEP numerical analysis/forecast products, satellite-derived precipitation (FY2) and digital elevation model (DEM) are used to produce 0.0625°, hourly estimates of meteorological forcing data by operating the Space-Time Multi-Scale Analysis System (STMAS) (Shi et al., 2014; Wang et al., 2021a). Meanwhile, the meteorological forcing is validated using national automatic station observations (more than 2400 stations). Second, the meteorological forcing is used to drive the multi-LSMs system to obtain a multi-layer ensemble of soil moisture estimates. Finally, the ensemble mean is applied to each soil layer to produce a soil moisture ensemble analysis product.

2.4.7 SMAP L4

The SMAP Level-4 soil moisture (L4-SM) is produced by assimilating SMAP radiometer Level 1C brightness temperature observations into CLSM and provides global, 3-hourly, 9-km resolution estimates of SSM (0-5 cm) and RZSM (0-100 cm) from March 2015 to present (Reichle et al., 2020; Reichle et al., 2021). The Goddard Earth Observation System, version 5, LDAS (GEOS-5 LDAS) uses a spatially distributed ensemble Kalman filter (EnKF) to assimilate the observations into CLSM (Rienecker et al., 2008). The EnKF has a 3-hourly update time step and is used to interpolate and extrapolate the brightness temperature and model estimates in time and space (Reichle et al., 2017a). The GEOS-5 CLSM is driven by surface meteorological data (precipitation, radiation, etc.) from the GEOS-5 Forward Processing (FP) system where large amounts of observations are assimilated into a global atmospheric model. The CPCU, 0.5-degree, daily precipitation observations are used to correct the GEOS-5 FP model background precipitation. Prior to the GEOS-5 FP precipitation correction, both the CPCU precipitation

https://doi.org/10.5194/egusphere-2023-1597
Preprint. Discussion started: 22 September 2023

data and the hourly background precipitation are scaled to the climatology of the GPCPv2.2 pentad precipitation product.

2.4.8 SMOS L4

The SMOS L4 soil moisture product is disseminated by SMOS CATDS and provides global, daily estimates of RZSM (0–100 cm) over a 25-km EASE-2 grid from January 2010 to present (Al Bitar and Mahmoodi, 2020; CATDS, 2021). The SMOS L4 RZSM is derived from the SMOS L3 3-day SSM product using a modified exponential filter linking the characteristic time length T (the transfer time of water from the surface layer to the root zone layer) to the soil properties (Pablos et al., 2018). The product is based on SMOS descending orbit (18:00) observations and other ancillary datasets such as MODIS observations, NCEP climate data and an updated FAO/UNESCO soil properties map. The soil column is divided into three layers (layer 1: 0-5 cm, layer 2: 5-40 cm, layer 3: 40-100 cm) in a water bucket model. The scaled 0-5 cm soil moisture is modified using a logarithmic function and filtered to obtain the layer 2 soil moisture. The scaled layer 2 soil moisture is then filtered using a different value of T to give the layer 3 soil moisture. Finally, the RZSM (0-100 cm) is calculated as a depth-weighted average of the soil moisture of the three layers (Al Bitar et al., 2021).

https://doi.org/10.5194/egusphere-2023-1597
Preprint. Discussion started: 22 September 2023

Table 1. Description of global and regional RZSM gridded products used in this study.

Dataset	Land surface model	Time period	resolution	Soil map	Soil layers	Data access
ERA5 (Global)	HTESSEL	January 1979-present	Hourly /0.25°	FAO	0-7 cm, 7-28 cm, 28-100 cm, 100-289 cm	ERA5 reanalysis datasets Hourly 0.25 x 0.25 degree| ECMWF
MERRA-2 V2.0 (Global)	CLSM	January 1980-present	Hourly /0.25°	FAO	0-5 cm, 0-100 cm	GES DISC Dataset: MERRA-2 tavg1_2d_lnd_Nx (M2T1NXLND 5.12.4) (nasa.gov)
NCEP CFSv2 V2.0 (Global)	Noah	January 2011-present	6-Hourly /0.20°	FAO	0-10 cm, 10-40 cm, 40-100 cm, 100-200 cm	CISL RDA: NCEP Climate Forecast System Version 2 (CFSv2) 6-hourly Products (ucar.edu)
GLDAS_NOAH V2.1 (Global)	Noah	January 2000-present	3-Hourly /0.25°	FAO	0-10 cm, 10-40 cm, 40-100 cm, 100-200 cm	GES DISC Dataset: GLDAS Noah Land Surface Model L4 3 hourly 0.25 x 0.25 degree V2.1 (nasa.gov)
GLDAS_CLSM V2.2 (Global)	CLSM	February 2003-present	Daily /0.25°	FAO	0-2 cm, 0-100 cm	GES DISC Dataset: GLDAS Catchment Land Surface Model L4 daily 0.25 x 0.25 degree GRACE-DA1 V2.2 (nasa.gov)
CLDAS V2.0 (Asia)	CLM CoLM Noah-MP	January 2008-present	Hourly /0.0625°	Shuangguan et al. (2013)	0-5 cm, 0-10 cm, 10-40 cm, 40-100 cm, 100-200 cm	China Meteorological Administration Land Data Assimilation System (CLDAS v2.0) Product Dataset (cma.cn)
SMAP Level 4 V5 (Global)	CLSM	March 2015-present	3-Hourly /9 km	HWSD	0-5 cm, 0-100 cm	SMAP L4 Global 3-hourly 9 km EASE-Grid Surface and Root Zone Soil Moisture Geophysical Data, Version 5 | National Snow and Ice Data Center (nsidc.org)
SMOS Level 4 V301 (Global)	Exponential filter (no LSM)	January 2010-present	Daily /0.25°	FAO	0-100 cm	L4 Land research products -Centre Aval de Traitement des Données SMOS (CATDS)

Note that precipitation, air temperature and soil texture have the same resolution as soil moisture.

https://doi.org/10.5194/egusphere-2023-1597
Preprint. Discussion started: 22 September 2023

3 Methods

3.1 Statistical metrics

Four widely used statistical metrics were used to quantitatively assess the performance of RZSM products against *in situ* measurements. The Pearson correlation coefficient (R) measures the linear correlation between the *in situ* measurements and the RZSM products. Mean Bias Error (MBE) reflects the mean systematic deviation of the model simulations relative to the measurements. Accuracy is assessed using the Root Mean Square Error (RMSE). The unbiased RMSE (ubRMSE) measures the standard deviation of the differences. In addition, Probability of Detection (POD), False Alarm Ratio (FAR) and Critical Success Index (CSI) are used to assess the ability of the global gridded rainfall to reproduce the measured rainfall (Su et al., 2019). In this study, these metrics are calculated at daily time steps after aggregating all sub-daily products to daily time steps. Note that the number of observations at each *in situ* station used to calculate the scores is 1827. The time series of different datasets (soil moisture, precipitation, air temperature and soil texture) are first averaged over all *in situ* stations and then used to calculate the metrics. The statistical metrics and corresponding formulas are listed in Table 2.

3.2 Calculation and validation of RZSM

As the *in situ* measurements are available at several specific depths (10, 20, 40 and 100 cm), the RZSM is calculated using a depth-weighted average of the four layers soil moisture layers (Xing et al., 2021). The equation is as follows:

$$\theta_{RZSM} = \frac{2\theta_1 L_1 + (\theta_1+\theta_2)L_2 + \cdots (\theta_{n-1}+\theta_n)L_n}{2(L_1+L_2+L_3+\cdots L_n)} \quad (1)$$

where θ_{RZSM} refers to the 0-100 cm RZSM ($m^3 m^{-3}$), θ_n is the volumetric soil moisture at the n_{th} observation depth ($m^3 m^{-3}$), and L_n is the soil layer thickness between adjacent observation depths (m).

For the RZSM products, in addition to the GLDAS_CLSM, MERRA-2, SMAP L4 and SMOS L4, which directly provide the 0-100 cm RZSM, other RZSM products are provided in different soil layers, NCEP CFSv2, CLDAS and GLDAS_NOAH (θ_{0-10c} , θ_{10-40} , $\theta_{40-100cm}$), ERA5 (θ_{0-7cm}, θ_{7-28} , $\theta_{28-100cm}$). For example, the GLDAS_NOAH RZSM can be calculated as:

$$\theta_{RZSM} = 0.1 \times \theta_{0-10cm} + 0.3 \times \theta_{10-40cm} + 0.6 \times \theta_{40-100cm} \quad (2)$$

https://doi.org/10.5194/egusphere-2023-1597
Preprint. Discussion started: 22 September 2023

Table 2. List of the statistical metrics for evaluation of RZSM products and corresponding precipitation forcing data using *in situ* measurements.

Statistic metrics	Unit	Equation	Optimal value
correlation coefficient (R)	-	$\frac{\sum_{i=1}^{n}(\theta_{est,i}-\overline{\theta_{est,i}})(\theta_{obs,i}-\overline{\theta_{obs,i}})}{\sqrt{\sum_{i=1}^{n}(\theta_{est,i}-\overline{\theta_{est,i}})^2}\sqrt{\sum_{i=1}^{n}(\theta_{obs,i}-\overline{\theta_{obs,i}})^2}}$	1
Mean Bias Error (MBE)	$m^3\ m^{-3}$	$\frac{\sum_{i=1}^{n}(\theta_{est,i}-\theta_{obs,i})}{n}$	0
Root Mean Square Error (RMSE)	$m^3\ m^{-3}$	$\sqrt{\frac{\sum_{i=1}^{n}(\theta_{est,i}-\theta_{obs,i})^2}{n}}$	0
unbiased Root Mean Square Error (ubRMSE)	$m^3\ m^{-3}$	$\sqrt{\frac{\sum_{i=1}^{n}\left((\theta_{est,i}-\overline{\theta_{est,i}})-(\theta_{obs,i}-\overline{\theta_{obs,i}})\right)^2}{n}}$	0
Probability of Detection (POD)	-	$\frac{H}{H+M}$	1
False Alarm Ratio (FAR)	-	$\frac{F}{H+F}$	0
Critical Success Index (CSI)	-	$\frac{H}{H+M+F}$	1
Normalized RZSM ($RZSM_{nor}$)	-	$\frac{RZSM-RZSM_{min}}{RZSM_{max}-RZSM_{min}}$	-

Note: n is the number of gap-filled daily observations (1827) used at each of the 58 *in situ* stations (see Table S1). $\theta_{est,i}$ and $\theta_{obs,i}$ are RZSM products and *in situ* measurements ($m^3\ m^{-3}$), respectively ; $\overline{\theta_{est,i}}$ and $\overline{\theta_{obs,i}}$ are the means of $\theta_{est,i}$ and $\theta_{obs,i}$ over the entire research period; H is the number of precipitation events detected by model and *in situ* measurements; M is the number of measured precipitation events not recognized by the model product; F is the number of model-based precipitation events not detected by *in situ* measurements. $RZSM_{nor}$ represents the normalized RZSM, $RZSM_{min}$ and $RZSM_{max}$ represent the maximum and minimum of RZSM, respectively.

https://doi.org/10.5194/egusphere-2023-1597
Preprint. Discussion started: 22 September 2023

4 Results

4.1 Comparison between gridded and *in situ* RZSM

Figure 2 shows scatterplots of RZSM products against the *in situ* measurements averaged across all in situ stations over the HRB, from 1 April 2015 to 31 March 2020. Regarding the bias, except for the underestimation by SMOS L4 (-0.047 $m^3 m^{-3}$), all the other products overestimate the RZSM observations by 0.030 $m^3 m^{-3}$ to 0.117 $m^3 m^{-3}$ (SMAP L4 and ERA5, respectively), especially for ERA5 and CLDAS. Due to the large bias, ERA5 and CLDAS have the largest RMSE values (0.122 and 0.114 $m^3 m^{-3}$, respectively) among all the RZMS products. Regarding correlation and ubRMSE, GLDAS_CLSM (R = 0.69, ubRMSE = 0.018 $m^3 m^{-3}$) outperforms the other RZSM products, followed by MERRA-2 (R = 0.58, ubRMSE = 0.023 $m^3 m^{-3}$), ERA5 (R = 0.58, ubRMSE = 0.033 $m^3 m^{-3}$), CLDAS (R = 0.56, ubRMSE = 0.023 $m^3 m^{-3}$), SMAP L4 (R = 0.53, ubRMSE = 0.027 $m^3 m^{-3}$) and GLDAS_NOAH (R = 0.54, ubRMSE = 0.030 $m^3 m^{-3}$), NCEP CFSv2 (R = 0.54, ubRMSE = 0.036 $m^3 m^{-3}$) and SMOS L4 (R = 0.35, ubRMSE = 0.027 $m^3 m^{-3}$). Overall, GLDAS_CLSM performs best among the eight RZSM products in terms of R, ubRMSE and bias values, while SMAP L4 presents the lowest RMSE and the lowest bias (0.040 and 0.030 $m^3 m^{-3}$, respectively). SMOS L4 presents the worst performance in terms of correlation with R = 0.35.

Figure 3 shows time series of *in situ* RZSM observations averaged over all in situ stations with its spatial variability, and of 3 RZSM products, ERA5, SMOS L4, and GLDAS_CLSM, presenting a marked overestimation, a marked underestimation, and the best overall agreement with *in situ* observations, respectively. Other products can be seen in Fig. S1. In general, all RZSM products capture the rapid temporal variations of the *in situ* soil moisture observations and correspond well to precipitation events, except for SMOS L4, which shows less rapid changes and smoother time series (Fig. 3 and Fig. S1). The *in situ* RZSM observations show a variation in the range of 0.1 to 0.4 $m^3 m^{-3}$. The range of NCEP CFSv2 and SMAP L4 RZSM is similar to the observed RZSM range. ERA5 and CLDAS present larger RZSM values, ranging from 0.2 to 0.5 $m^3 m^{-3}$. MERRA-2, GLDAS_CLSM and GLDAS_NOAH RZSM values range from 0.2 to 0.4 $m^3 m^{-3}$, which is a narrower interval compared to the other products. SMOS L4 displays the smallest RZSM values, ranging from 0.1 to 0.3 $m^3 m^{-3}$. The statistical distribution of the scores for the eight RZSM products against the *in situ* soil moisture observations at individual stations is shown in Fig. S2 and Table S1. Overall, the average score values in Table S1 are not as good as results shown in Table 3. In order to eliminate the seasonal effects and to examine the ability of the products to represent the daily variability of the RZSM, a five-week moving average window is used to calculate the monthly anomaly time series of the RZSM. Figure S3 displays a comparison of the results for monthly anomalies. In general, the performance of the eight RZSM products is better during the wet season than for the full annual cycle and the dry season (see Table S1).

https://doi.org/10.5194/egusphere-2023-1597
Preprint. Discussion started: 22 September 2023

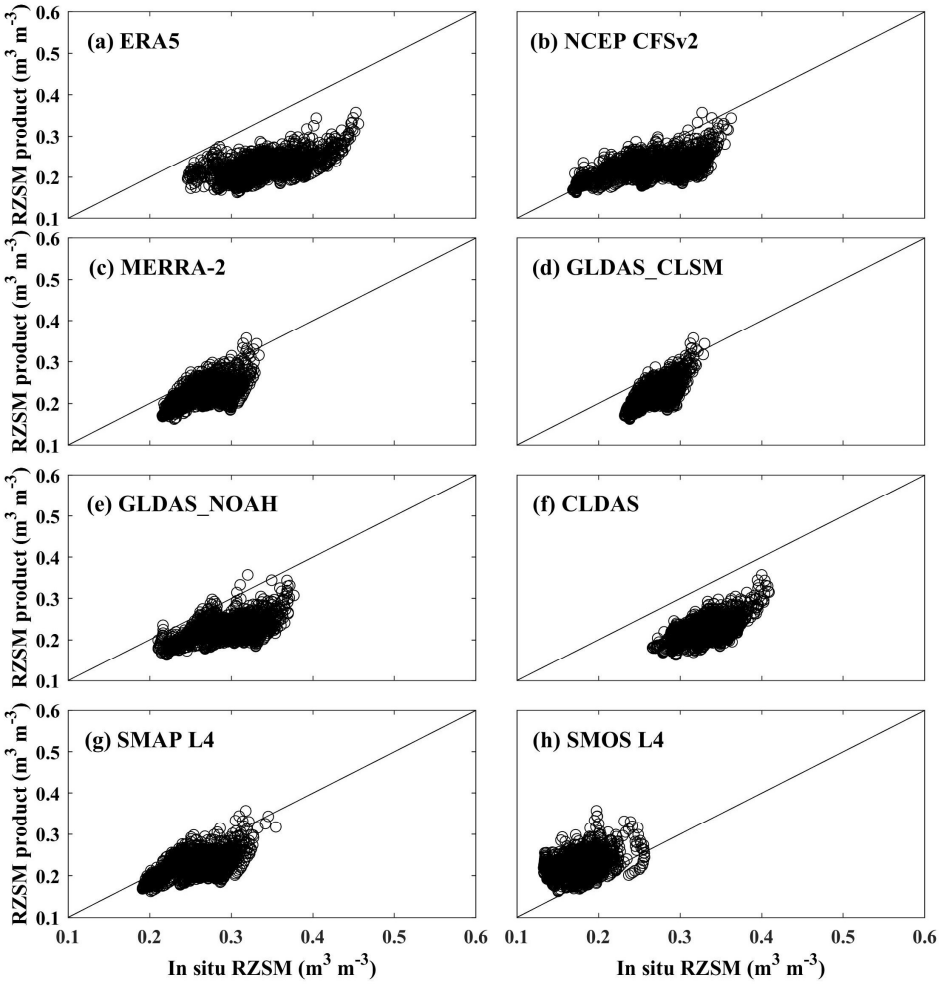

Fig. 2 Scatterplots of RZSM products vs. *in situ* RZSM observations averaged across all in situ stations from 1 April 2015 to 31 March 31 2020. Scores are given in Table 3.

https://doi.org/10.5194/egusphere-2023-1597
Preprint. Discussion started: 22 September 2023

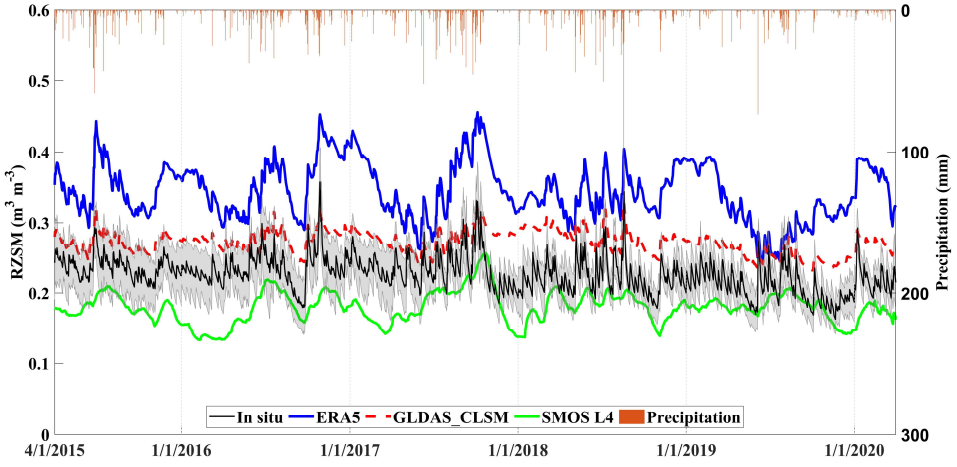

Fig. 3 Time series of RZSM (0-100 cm) products and *in situ* soil moisture observations averaged across all in situ stations from 1 April 2015 to 31 March 31 2020. ERA-5, GLDAS_CLSM and SMOS L4 are shown, other products can be seen in Fig. S1. The dark line and the gray-shaded areas represent the mean and standard deviation of *in situ* stations observations. ERA-5, GLDAS_CLSM and SMOS L4 are represented by the blue line, the dashed red line, the green line, respectively. Daily precipitation is represented by the orange vertical bars.

Table 3. Statistical metrics of eight RZSM products validated by *in situ* measurements (0-100 cm) averaged over all stations from 1 April 2015 to 31 March 2020 (Fig. 2). Mean score values are given. Best score values are in bold. The number of observations used to calculate the scores is 1827 for each product.

Dataset	*In situ* validation			
	R	Bias ($m^3 m^{-3}$)	RMSE ($m^3 m^{-3}$)	ubRMSE ($m^3 m^{-3}$)
ERA-5	0.58	0.117	0.122	0.033
MERRA-2	0.58	0.040	0.046	0.023
NCEP CFSv2	0.54	0.041	0.055	0.036
GLDAS_NOAH	0.54	0.071	0.077	0.030
GLDAS_CLSM	**0.69**	0.046	0.049	**0.018**
CLDAS	0.56	0.107	0.114	0.023
SMAP L4	0.53	**0.030**	**0.040**	0.027
SMOS L4	0.35	-0.047	0.055	0.027

https://doi.org/10.5194/egusphere-2023-1597
Preprint. Discussion started: 22 September 2023

4.2 Intercomparison of gridded RZSM products

Figure 4 displays the pairwise comparison of the eight RZSM products for grid cells located above the *in situ* stations. Overall, there is good agreement between all RZSM products, except for SMOS L4. The correlation coefficient *R* between each of the other seven RZSM products varies from 0.30 (MERRA-2 versus SMOS L4) to 0.95 (SMAP L4 versus MERRA-2), with an average value of 0.71. The mean bias varies from -0.067 $m^3 m^{-3}$ (MERRA-2 minus CLDAS) to 0.165 $m^3 m^{-3}$ (ERA5 minus SMOS L4), with an average value of 0.037 $m^3 m^{-3}$. The ubRMSE varies from 0.010 $m^3 m^{-3}$ (MERRA-2 versus SMAP L4) to 0.040 $m^3 m^{-3}$ (NCEP CFSv2 versus SMOS L4), with an average value of 0.024 $m^3 m^{-3}$. SMOS L4 differs most from the other products. The correlation coefficient *R* between SMOS L4 and the other seven RZSM products varies from 0.30 (MERRA-2 vs. SMOS L4) to 0.41 (GLDAS_NOAH versus SMOS L4), with an average value of 0.35, and the mean bias varies from 0.077 $m^3 m^{-3}$ (SMAP L4 minus SMOS L4) to 0.165 $m^3 m^{-3}$ (ERA5 minus SMOS L4), with an average value of 0.112 $m^3 m^{-3}$. The ubRMSE varies from 0.023 $m^3 m^{-3}$ (GLDAS_CLSM versus SMOS L4) to 0.400 $m^3 m^{-3}$ (NCEP CFSv2 versus SMOS L4), with an average value of 0.031 $m^3 m^{-3}$.

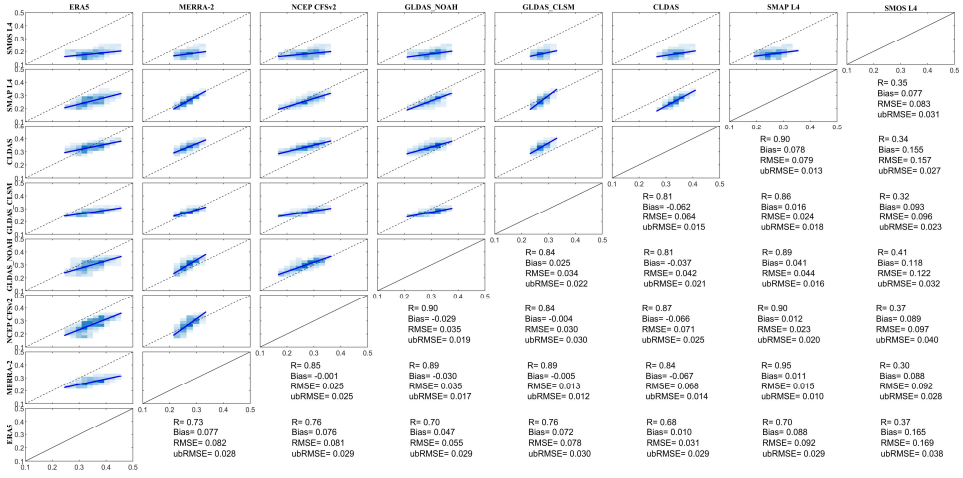

Fig. 4 Comparison of different RZSM products (volumetric water content, $m^3 m^{-3}$) with each other. The scatterplots and their corresponding statistics are located on opposite sides of each other, that is, the scatterplot of the data pair SMOS L4-ERA5 is in the top left-hand corner, while the respective statistical values are found in the bottom right-hand corner. Darker regions show a higher density of data point.

Figure 5 shows the histograms of normalised RZSM of the eight products and the *in situ* observations. The relative frequency distribution corresponding to the normalized soil moisture interval varies considerably between the different RZSM datasets. All soil moisture datasets are almost normally distributed with a clear peak. However, the observed RZSM distribution is skewed towards low values, and the most frequent normalised RZSM class falls in the range of 0.3 to 0.4. The MERRA-2, GLDAS_CLSM, SMAP L4, and ERA5 products exhibit the same behaviour. In contrast, SMOS L4, NCEP CFSv2 and CLDAS display a relative frequency peak in the range of 0.4

https://doi.org/10.5194/egusphere-2023-1597
Preprint. Discussion started: 22 September 2023

to 0.5. GLDAS_NOAH, on the other hand, shows a peak in the range of 0.5 to 0.6, and is clearly skewed towards the wetter end of the distribution.

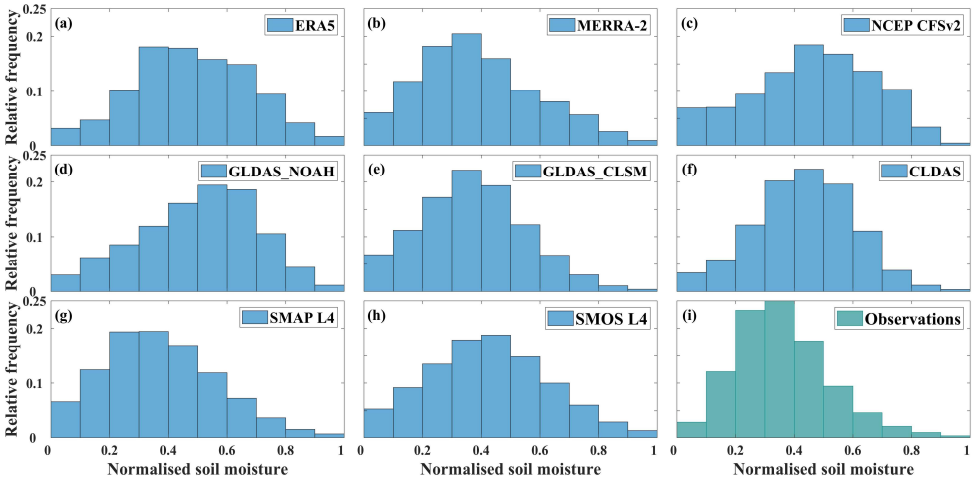

Fig. 5 Histograms showing the relative frequency (vertical axis) of the various normalized RZSM datasets and *in situ* observations.

4.3 Validation of atmospheric forcings and soil properties

4.3.1 Precipitation and air temperature

Figure 6 shows the differences between the model and ground-based precipitation. A daily precipitation amount of less than 1 mm is considered as a no-rain criterion. During the period from 1 April 2015 to 31 March 2020, the annual mean precipitation amount from global products (SMAP: 1024 mm yr^{-1}, GLDAS_NOAH: 988 mm yr^{-1}, GLDAS_CLSM: 986 mm yr^{-1}, MERRA-2: 974 mm yr^{-1}, NCEP CFSv2: 951 mm yr^{-1}, ERA5: 880 mm yr^{-1}) overestimate the ground-based observations (840 mm yr^{-1}) by 22, 18, 17, 16, 13, and 5 %, respectively. In addition, the mean frequency of rainy days (131, 114, 114, 113, 114, 126 d yr^{-1}) is larger than observed (97 d yr^{-1}) due to the drizzle effect often produced by AGCM (Piani et al., 2010; Velasquez et al., 2020). In contrast to the global products mentioned above, CLDAS (806 mm yr^{-1}) slightly underestimates the mean annual precipitation amount by 4 %, and the precipitation frequency (99 days yr^{-1}) is close to the ground-based observation. Furthermore, the global precipitation products tend to underestimate the *in situ* precipitation observations for precipitation events above 50 mm d^{-1} (Fig. 6). Overall, the precipitation products are in good agreement with the observed precipitation, with *R* values generally above 0.4 (left panel of Fig. 7). MERRA-2, ERA5, GLDAS_CLSM, and SMAP L4 show strong ability to detect precipitation with POD value above 0.6 (right panel of Fig. 7). The *R* value between modelled and ground-based precipitation is directly related to the CSI value except for GLDAS_NOAH.

https://doi.org/10.5194/egusphere-2023-1597
Preprint. Discussion started: 22 September 2023

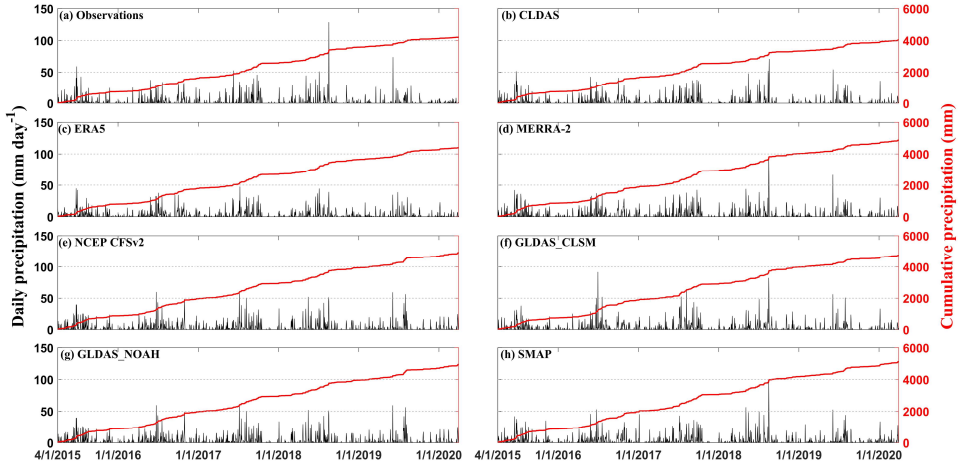

385 **Fig. 6 Comparison of daily precipitation and cumulative precipitation time series between model-derived precipitation and in situ precipitation observations averaged over all *in situ* stations.**

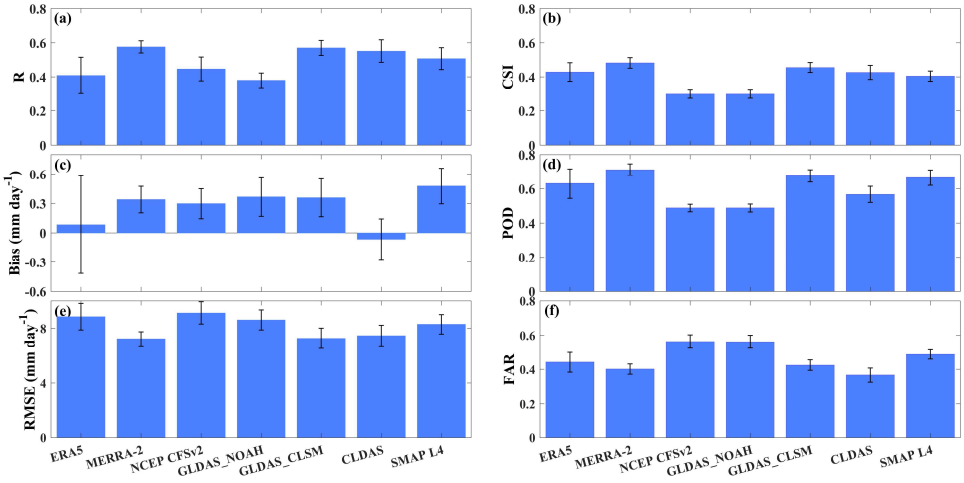

390 **Fig. 7 Summary of error metrics of gridded precipitation data against *in situ* precipitation observations (left panel), right panel shows the detection ability of gridded precipitation to reproduce the observed precipitation. The blue histogram represents the median and black error bar represents the standard deviation.**

The daily air temperature data derived from ERA5, MERRA-2, NCEP CFSv2, GLDAS_CLSM, CLDAS, 395 GLDAS_NOAH and SMAP L4 are validated against *in situ* observations of daily air temperature after aggregating all sub-daily products to daily time steps. Figures 8 and S4 shows that the modelled air temperature captures the observed temporal variation well, with *R* values above 0.96. However, all of them show underestimation, indicated by negative bias values ranging from -4.0 to -5.2 K (Table 4).

https://doi.org/10.5194/egusphere-2023-1597
Preprint. Discussion started: 22 September 2023

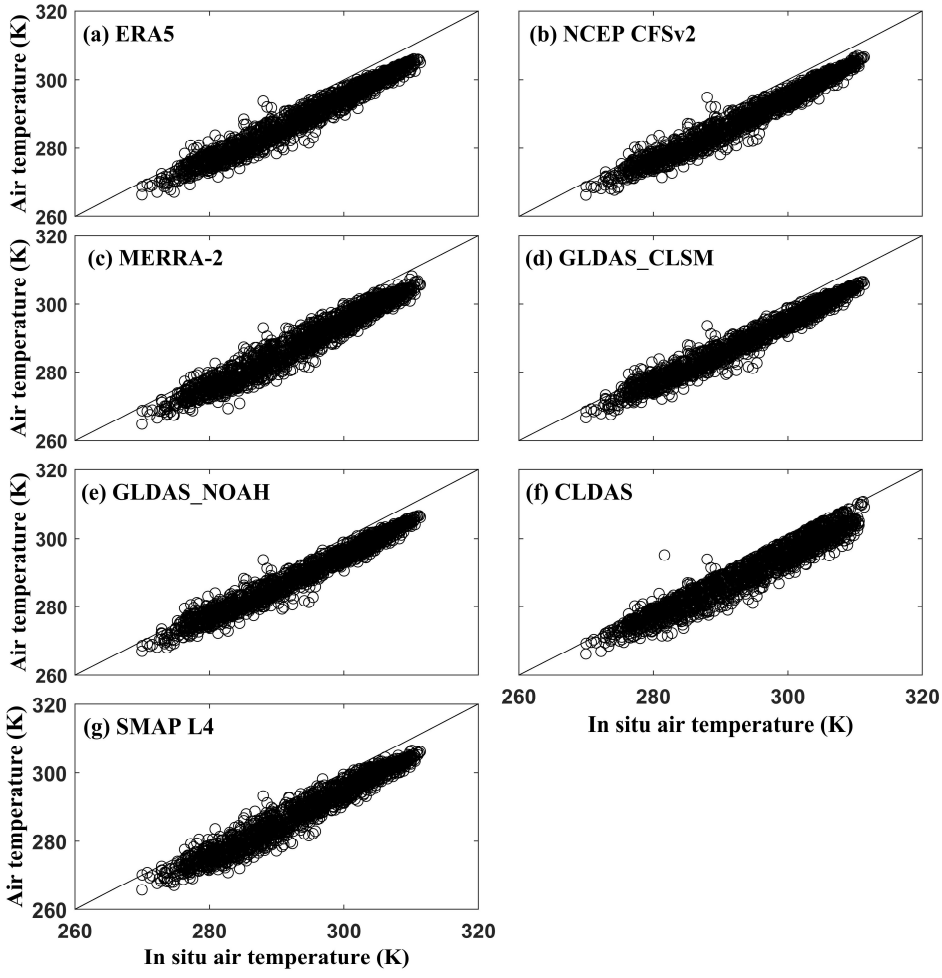

400 **Fig. 8 Scatterplots of model- and observation-based air temperature averaged over all stations, from 1 April 2015 to 31 March 2020. ERA5, MERRA-2, NCEP CFSv2, GLDAS_CLSM, GLDAS_NOAH, CLDAS and CMA products provide the air temperature datasets at the 2-m screen level. SMAP L4 product provides the air temperature at center height of the lowest atmospheric model layer.**

https://doi.org/10.5194/egusphere-2023-1597
Preprint. Discussion started: 22 September 2023

Table 4. Statistical metrics of air temperature products validated by *in situ* measurements averaged over all stations from 1 April 2015 to 31 March 2020. Mean score values are given. Best score values are in bold. The number of observations used to calculate the scores is 1827 for each product.

Dataset	*In situ* validation			
	R	Bias (K)	RMSE (K)	ubRMSE (K)
ERA-5	0.98	-4.8	5.2	2.1
MERRA-2	0.98	-5.1	5.7	2.4
NCEP CFSv2	0.98	-4.9	5.3	2.1
GLDAS_NOAH	0.98	-4.3	4.8	2.1
GLDAS_CLSM	0.98	-4.5	4.9	2.1
CLDAS	0.96	-4.0	4.9	2.8
SMAP L4	0.97	-5.2	5.7	2.4

4.3.2 Soil properties

In this study, four soil properties indicators, including clay and sand content, organic carbon content and bulk density were selected to investigate the differences among the FAO/UNESCO soil map of World, HWSD, and the reference soil dataset developed by Shangguan et al. (2013). The soil properties data used in the eight RZSM products were all derived from the FAO/UNESCO soil map of World except for CLDAS, which used the soil data developed by Shangguan et al. (2013), and SMAP L4, which used the HWSD soil properties over China. Figure 9 shows the reference dataset and HWSD generally exhibit similar properties, although the reference dataset has slightly higher organic carbon content and lower sand content. Both of them differ from the FAO/UNESCO soil properties data. FAO/UNESCO overestimates the clay content for the upper (0-30 cm) and lower (30-100 cm) soil layers. Sand content is also overestimated for the subsurface layer but it is underestimated for the surface layer.

https://doi.org/10.5194/egusphere-2023-1597
Preprint. Discussion started: 22 September 2023

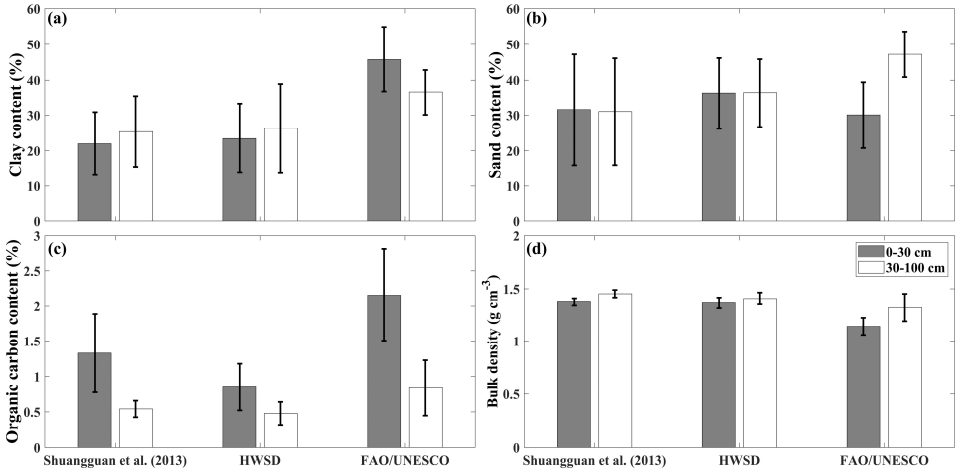

Fig. 9 Comparison of three sets of soil properties data (FAO used in ERA5, MERRA2, NCEP CFSv2, GLDAS_NOAH, GLDAS_CLSM and SMOS), HWSD used in SMAP L4 and reference soil properties data Shangguan et al. (2013) used in CLDAS. The histogram (gray bar: 0-30 cm; white bar: 30-100 cm) represents the median and black error bar represents the standard deviation.

https://doi.org/10.5194/egusphere-2023-1597
Preprint. Discussion started: 22 September 2023

5 Discussion

5.1 What is the impact of uncertainties of meteorological forcing data?

The accuracy of LSM simulations is influenced by the quality of the meteorological forcing, which is considered to be one of the most important and direct factors, especially precipitation and air temperature (Reichle et al., 2012; Yang et al., 2020; Zeng et al., 2021). Global precipitation and air temperature forcing data are used in the production of all RZSM products except for SMOS L4. These forcing data are compared with reference data extracted from the China gridded precipitation and air temperature dataset. The larger amount and frequency of precipitation (Fig. 6) could be a reason for the overestimation of soil water storage by RZSM products. We also quantitatively evaluated the gridded precipitation by comparing it to ground-based precipitation to investigate the effect of precipitation accuracy on the performance of RZSM products (Fig. 6). In terms of *R*, RMSE, CSI, POD and FAR, MERRA-2 and GLDAS_CLSM precipitation are the best performing products. This may explain the relatively better agreement of MERRA-2 and GLDAS_CLSM RZSM with *in situ* data in terms of correlation (Table 3). For most reanalysis products, the precipitation used to drive the different LSMs was generated by the AGCM through the assimilation of atmospheric temperature, humidity and wind observations (Reichle et al., 2017c). The MERRA-2 model background precipitation corrected with NOAA CPCU gauge-based precipitation observations before driving the land surface water budget was implemented in the coupled land-atmosphere reanalysis system, which may also contribute to the high consistency with the ground-based precipitation. Being driven by *in situ* precipitation observations, the CLDAS multi-LSMs should have produced RZSM values close to the observations. However, the CLDAS RZSM product overestimates the *in situ* observations by 0.107 $m^3 m^{-3}$ (Table 3). Therefore, precipitation may not be the dominant factor contributing to the overestimation of RZSM for the CLDAS RZSM (Bi et al., 2016; Qin et al., 2017).

Air temperature is another key factor in determining the accuracy of RZSM simulations, as it controls soil evaporation and plant transpiration. The underestimation of air temperature by reanalyses has been illustrated in previous studies (Wang and Zeng, 2012; Yang et al., 2020). In general, the lower air temperature results in less evapotranspiration, and more soil water storage. This is consistent with the overestimation of *in situ* observations by LSM-based RZSM products (Bi et al., 2016; Yang et al., 2020). Compared to precipitation, air temperature has an overall better correlation with *in situ* observations. Note that ERA5 includes an analysis of soil moisture and screen-level (2 m) air temperature and air humidity. Studies have indicated that the assimilation of screen-level variables improves root zone soil moisture estimates relative to *in situ* observations providing more realistic lower boundary conditions for numerical prediction models (Douville et al., 2000; Seuffert et al., 2003; de Rosnay et al., 2012). The overestimation of RZSM by ERA5 (Fig. 3) could be a signature of irrigation because the *in situ* RZSM observations do not capture irrigation.

5.2 Are soil properties correctly represented?

Time-invariant soil property data (e.g. porosity) are key model parameters for LSMs because they determine the physical structure of the soil in the vadose zone, which controls the partitioning of precipitation into surface runoff and infiltration. In general, soil texture is closely related to the ability of the soil to retain water, as water molecules adhere more tightly to fine-textured clay particles than coarse-textured sand particles. Consequently,

https://doi.org/10.5194/egusphere-2023-1597
Preprint. Discussion started: 22 September 2023

clay exhibits stronger water retention capacity and higher water content stored in the soil compared to sand at the same matric potential. In addition, the overestimated FAO/UNESCO soil organic carbon content (Fig. 9) leads to higher soil porosity and lower bulk density. As a result, water can infiltrate more quickly and more water can flow through the soil and can be retained in the soil (Bot and Benites, 2005; Reichle et al., 2017b). Therefore, the use of inaccurate FAO/UNESCO soil property data used in LSMs may explain the overestimation of soil moisture by the various RZSM products compared to the ground-based observations. It is promising to improve the accuracy of LSM-based RZSM using HWSD instead of FAO/UNESCO soil property data.

Soil stratification can affect the accuracy of LSM-based RZSM by impeding the water transfer from the surface layer to the root zone layer. In the Huaibei plain, the soil column can basically be divided into three layers, including the plough layer (0–16.6 cm), the black soil layer (16.6–49.3 cm) and the lime concretion layer (49.3–138.3 cm) due to the long-term human activities (e.g. fertilisation and ploughing), which significantly increases the soil organic carbon content and porosity in the plough layer compared to the deeper soil layer (Zhang et al., 2001; Li et al., 2011; Zha et al., 2015; Gu et al., 2021). There is a noticeable difference in soil properties between the plough layer and the black soil layer, while the difference between the black soil layer and the lime concretion layer is relatively small (see Fig. S5). High porosity results in high hydraulic conductivity and infiltration capacity (Zha et al., 2015). Therefore, interflow can occur due to the difference of infiltration rate between adjacent soil layers. The interflow may either flow horizontally due to good lateral drainage conditions or accumulate vertically and evaporate. These processes may not be well represented by LSMs.

In the study by Fan et al. (2022), RZSM products (SMAP-L4 V6, ERA5-land V2, GLDAS-Noah V2.1) were evaluated over croplands in Jiangsu province, which is close to the Huaibei Plain. A fourth RZSM dataset was derived from the ESA CCI SSM using an exponential filter. In this study, SMAP L4, ERA5 and GLDAS_NOAH overestimate the *in situ* RZSM. Overall, both studies show similar *R* values of RZSM products against the *in situ* observations, but with opposite biases. The changes in the sign of the bias could be attributed to differences in soil properties. In the Huaibei plain, the main soil type is lime concretion black soil, whose main characteristic are (1) soil stratification, (2) poor soil permeability and water retention capacity due to high clay content, (3) clay swelling during wet periods and shrinking during dry periods. During drought, cracks in the soil column increase and deepen, resulting in capillary breakage and increased evaporation. During wet periods, the soil absorbs water and swells, closing the cracks and preventing water infiltration. Water is then lost mainly through surface runoff. This could explain the lower RZSM values ranging from 0.2 to 0.3 $m^3 m^{-3}$ observed in the Huaibei plain and the higher RZSM values ranging from 0.3 to 0.4 $m^3 m^{-3}$ observed in Jiangsu. The larger amount of precipitation in Jiangsu could be another possible reason.

5.3 What are the difference between the three CLSM-based RZSM products?

Regarding the *in situ* validation in Sect. 4.1, the superior skill metrics of GLDAS_CLSM among the three CLSM-based RZSM products (GLDAS_CLSM, SMAP L4 and MERRA-2), can be attributed to its more accurate representation of precipitation. While GRACE TWS observations have been assimilated into GLDAS_CLSM, previous studies have indicated that the assimilation of GRACE TWS has no or negligible effect on RZSM. This could be attributed to the faster response of soil moisture to atmospheric forcing than groundwater (Zaitchik et al., 2008; Houborg et al., 2012; Girotto et al., 2016), the short *in situ* data record or insufficient spatial sampling (Li et al., 2012). Tian et al. (2017) and Tangdamrongsub et al. (2020) jointly assimilated terrestrial water storage

https://doi.org/10.5194/egusphere-2023-1597
Preprint. Discussion started: 22 September 2023

(GRACE TWS) and SSM products. The soil moisture-only assimilation improved the performance of soil moisture estimates relative to *in situ* measurements but degraded the performance of groundwater estimates. The GRACE-only assimilation only enhanced the skill metrics of groundwater estimates.

Regarding the intercomparison in Sect. 4.2, the very good correlation and low ubRMSE between MERRA-2 and SMAP L4 shown in Fig. 4 can be partly attributed to the fact that both products are based on the CLSM and both use atmospheric forcing data generated from GEOS-5. However, it should be noted that SMAP L4 uses a more recent version of CLSM with a different representation of soil hydraulic and thermal properties. In addition, MERRA-2 and SMAP L4 use different model background precipitation (i.e. GEOS-5 FP system for SMAP L4 and GEOS-5 FP-IT system for MERRA-2) (Reichle et al., 2017c). In MERRA-2, the CPCU precipitation is used in its native climatology to correct the GEOS FP-IT model background precipitation, while in SMAP L4 the CPCU precipitation is rescaled to the climatology of the GPCPv2.2 pentad precipitation product climatology before being corrected by the GEOS-5 FP system. De Lannoy et al. (2014) showed that SMAP L4 has a smaller mean bias in SSM and RZSM than MERRA-2 due to the increased sand content of the HWSD and the new pedotransfer functions provided by Wösten et al. (2001), which is consistent with result of this study.

5.4 How does the mismatch of spatial scales affect the evaluation results?

In addition to the model- and the observation-based soil moisture errors, the mismatch of spatial scales between grid-scale soil moisture simulations and point-scale observations also introduces additional errors. As shown in the statistical metrics shown in Tables 3 and S1, the *R* and ubRMSE values calculated on regional scale are generally better than those calculated on point scale. For the latter comparison, the grid-based RZSM lacks representativeness of soil moisture within the grid cell due to the high spatial variability resulting from different characteristics of the underlying surface and meteorological forcing. This leads to an error in representativeness (Xia et al., 2014). In contrast, the former comparison improves the representativeness of the grid-based RZSM and reduces the spatial noise (Wang and Zeng, 2012; Xia et al., 2014; Bi et al., 2016; Zheng et al., 2022). In addition, upscaling the sparse ground-based observations to the footprint-scale satellite soil moisture retrieval or model grid scale through the temporal stability concept, block kriging, field campaign data, or LSM, reduces the uncertainty of spatial resampling and further improves the reliability of soil moisture validation (Crow et al., 2012).

5.5 Why does SMOS L4 underestimate RZSM?

The SMOS L4 RZSM is derived from the SMOS L3 3-day SSM by applying a modified exponential filter (Pablos et al., 2018). Figure 10 shows the comparison of the SMOS L3 SSM and L4 RZSM with the *in situ* soil moisture observations. It is evident that both SMOS L3 SSM and L4 RZSM underestimate the *in situ* observations with average bias values of -0.069 and -0.047 $m^3 m^{-3}$, respectively. By partitioning the total error composed of the exponential filter model and the inherent SMOS *in situ* differences, Ford et al. (2014) have shown that the mismatch between *in situ* observations and the estimates is much larger than the error caused by the exponential filter method. The underestimation of *in situ* observations by SMOS L3 SSM has been reported in previous studies (Djamai et al., 2015; Cui et al., 2017; Pablos et al., 2018; Ma et al., 2019; Wang et al., 2021b). Therefore, it can be inferred that the underestimation of *in situ* observations by the SMOS L3 SSM propagates to the SMOS L4 RZSM. The L-band microwave signal is sensitive to soil moisture, soil temperature and vegetation optical depth (VOD) (Kerr et al., 2012). Using the L-band Microwave Emission of the Biosphere (L-MEB) model (Wigneron

https://doi.org/10.5194/egusphere-2023-1597
Preprint. Discussion started: 22 September 2023

et al., 2021), SMOS L3 soil moisture and Vegetation Optical Depth (VOD) can be retrieved simultaneously from multiple orbits using multi-angular (~0-60°) and dual-polarisation TB measurements (Al Bitar et al., 2017; Li et al., 2021). Numerous studies have shown that the SMOS L3 physical surface temperature used in the forward radiative transfer model was underestimated (Cui et al., 2017; Ma et al., 2019; Wang et al., 2021b; Zheng et al., 2022). In the SMOS L3 retrieval algorithm, underestimation of soil temperature leads to overestimation of soil emissivity, which ultimately results in the underestimation of soil moisture retrieval. In general, the SMOS L3 VOD retrievals are relatively noisy, which may be related to retrieval instabilities and Radio Frequency Interference (RFI) effects (Cui et al., 2017; Wang et al., 2021b; Wigneron et al., 2021; Zheng et al., 2022). Therefore, it is difficult to quantify its relationship with soil moisture. In addition, the ECMWF ERA-Interim soil moisture is also used in the operational SMOS L3 SSM retrieval algorithm. For a given pixel, the total TB is simulated as the sum of several fractional contributions (F_{NO}: nominal (bare soil, low vegetation), F_{FO}: forest, and others as urban, water, etc.), i.e. $TB_{total} = TB_{FNO} + TB_{FFO} + TB_{others}$ (Fernandez-Moran et al., 2017). SMOS L3 retrievals are computed only over a fraction of the pixel (the "dominant" fraction where SM retrieval is meaningful over certain surface types) (Fernandez-Moran et al., 2017; Wigneron et al., 2021). For the remaining fraction of pixels, only their contributions to the total signal need to be estimated using the ECMWF ERA-Interim SM (0-7 cm) as an auxiliary input, but no SM retrievals are performed. Previous studies have shown that the ERA-Interim soil moisture over China is overestimated (Yang et al., 2020; Ling et al., 2021). Therefore, the overestimated ECMWF ERA-Interim SM (0-7 cm) leads to an underestimation of the forest TB_{FFO} contribution, which in turn leads to an overestimation of TB_{FNO} and to a dry bias in the retrieved SMOS L3 SM (as there is a negative correlation between brightness temperature and soil moisture (Rao et al., 2007)).

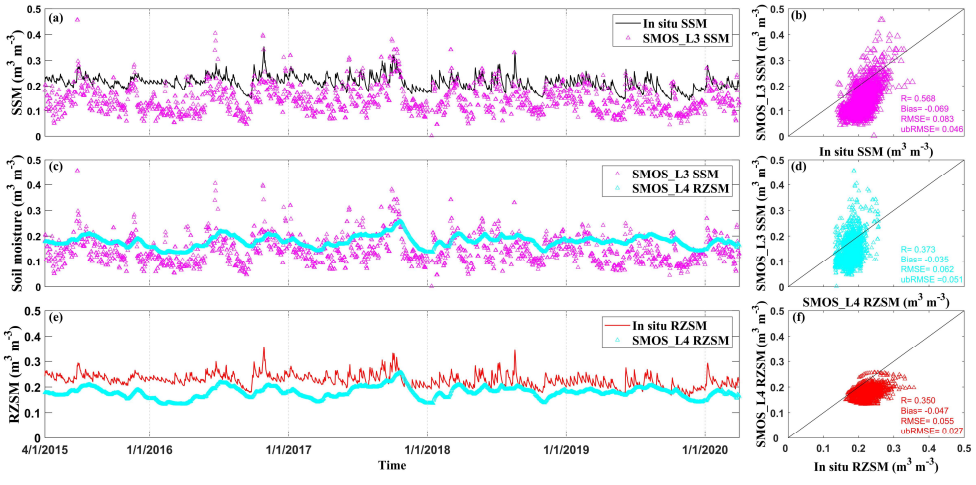

Fig. 10 Comparison of time series (left panel) and scatterplots (right panel) of SMOS L3 SSM vs. *in situ* SSM (Fig. 10a and b), SMOS L3 SSM vs. SMOS L4 RZSM (Fig. 10c and d) and SMOS L4 RZSM vs. *in situ* RZSM (Fig. 10e and f).

https://doi.org/10.5194/egusphere-2023-1597
Preprint. Discussion started: 22 September 2023

6 Conclusion

In this study, eight RZSM products were quantitatively evaluated against observations from 58 *in situ* soil moisture stations over the heavily irrigated HRB in China. Statistical metrics of *R*, mean bias, RMSE and ubRMSE were used to evaluate the performance of different RZSM products. The impact of several potential confounding factors on the uncertainty of RZSM products was investigated. These factors included meteorological forcing variables (precipitation and air temperature), soil properties (organic matter, bulk density, clay and sand content), soil stratification and spatial scale mismatch. The main conclusions of this study are as follows:

(1) GLDAS_CLSM performed best among the RZSM products based on LSMs over the HRB in terms of *R*, ubRMSE and mean bias, followed by MERRA-2, CLDAS, SMAP, ERA5, NCEP CFSv2, and GLDAS_NOAH. The SMOS L4 product presented the worst performance. All LSM-based products overestimated the RZSM with median bias values ranging from 0.033 $m^3 m^{-3}$ (SMAP L4) to 0.116 $m^3 m^{-3}$ (CLDAS). On the other hand, SMOS L4 underestimated the RZSM with a median bias value of -0.050 $m^3 m^{-3}$. ERA5 and CLDAS had the largest biases, of 0.104 $m^3 m^{-3}$ and 0.116 $m^3 m^{-3}$, respectively. However, the ERA5 screen-level parameters analysis could indirectly account for irrigation.

(2) The correlation coefficient *R* between any two of the seven LSM-based RZSM products varied from 0.68 (ERA5 vs. CLDAS) to 0.95 (SMAP L4 vs. MERRA-2). SMOS L4 did not correlate well with the other seven RZSM products with *R* ranging from 0.30 (MERRA-2) to 0.41 (GLDAS_NOAH) and with a negative bias ranging from -0.165 $m^3 m^{-3}$ (SMOS L4 minus ERA5) to -0.077 $m^3 m^{-3}$ (SMOS L4 minus SMAP L4).

(3) Precipitation may be the most important factor in determining the accuracy of LSM-based RZSM. With the exception of CLDAS, the different precipitation datasets all show an overestimation of total precipitation and precipitation frequency (excessive number of occurrences of drizzle events). This may explain the overestimation of *in situ* soil moisture observations by various RZSM products, but not for CLDAS. The air temperature used to drive the LSMs had a cold bias ranging from -4.0 K (CLDAS) to -5.19 K (SMAP L4), which tended to decrease evapotranspiration and increase RZSM.

(4) The underestimation of the SMOS L4 RZSM may be related to the underestimation of the SMOS L3 SSM.

https://doi.org/10.5194/egusphere-2023-1597
Preprint. Discussion started: 22 September 2023

Data availability. The soil moisture observations in Huai River Basin is not publicly available but could be requested from the Huaihe River Commission of the Ministry of Water Resources, P. R. C. (https://hrc.gov.cn). We provide a sample data set of these measurements for a subset of 10 stations (https://doi.org/10.6084/m9.figshare.23497502). The soil moisture time series of the 10 in situ stations can be seen in Fig. S6.

Author contributions. EL, YHZ, JCC and HSL conceptualized the project. EL led the investigation, determined the methodology and wrote the original draft of the paper. All the co-authors contributed to the review and editing of the paper.

Competing interests. The authors declare that they have no conflict of interest.

Disclaimer. Publisher's note: Copernicus Publications remains neutral with regard to jurisdictional claims in published maps and institutional affiliations.

Acknowledgement. We acknowledge the European Centre for Medium-Range Weather Forecasts (ECMWF), Goddard Earth Sciences Data and Information Services Center (GES DISC), National Center for Atmospheric Research (NCAR), China Meteorological Administration (CMA), National Snow & Ice Data Center (NSIDC) and Centre Aval de Traitement des Données (CATDS) for providing data free of charge.

Financial support. This research was funded by National Key Research and Development Program (grant nos. 2019YFC1510504); National Natural Science Foundation of China (grant nos. 41830752, 42071033 and 41961134003).

https://doi.org/10.5194/egusphere-2023-1597
Preprint. Discussion started: 22 September 2023

References

610 Al Bitar, A. and Mahmoodi, A.: Algorithm Theoretical Basis Document (ATBD) for the SMOS Level 4 Root Zone Soil Moisture (Version v30_01), Zenodo, http://doi.org/10.5281/zenodo.4298572, 2020.

Al Bitar, A., Mahmoodi, A., Kerr, Y., Rodriguez-Fernandez, N., Parrens, M. and Tarot, S.: Global Assessment of Droughts in the Last Decade from SMOS Root Zone Soil Moisture, 2021 IEEE International Geoscience and Remote Sensing Symposium (IGARSS) , 8628-8631, https://doi.org/10.1109/igarss47720.2021.9554773, 2021.

615 Al Bitar, A., Mialon, A., Kerr, Y. H., Cabot, F., Richaume, P., Jacquette, E., Quesney, A., Mahmoodi, A., Tarot, S., Parrens, M., Al-Yaari, A., Pellarin, T., Rodriguez-Fernandez, N. and Wigneron, J.-P.: The global SMOS Level 3 daily soil moisture and brightness temperature maps, Earth Syst. Sci. Data, 9, 293-315, https://doi.org/10.5194/essd-9-293-2017, 2017.

Albergel, C., Rüdiger, C., Pellarin, T., Calvet, J.-C., Fritz, N., Froissard, F., Suquia, D., Petitpa, A., Piguet, B. and Martin, E.: From near-surface to root-zone soil moisture using an exponential filter: an assessment of the method based on in-situ observations and model
620 simulations, Hydrol. Earth Syst. Sci., 12, 1323-1337, https://doi.org/10.5194/hess-12-1323-2008, 2008.

Babaeian, E., Sadeghi, M., Jones, S. B., Montzka, C., Vereecken, H. and Tuller, M.: Ground, Proximal, and Satellite Remote Sensing of Soil Moisture, Rev. Geophys., 57, 530-616, https://doi.org/10.1029/2018rg000618, 2019.

Beaudoing, H., Rodell, M. and NASA/GSFC/HSL: GLDAS Noah Land Surface Model L4 3 hourly 0.25 x 0.25 degree V2.1, , Greenbelt, Maryland, USA, Goddard Earth Sciences Data and Information Services Center (GES DISC), Accessed: [Data Access Date],
625 https://doi.org/10.5067/E7TYRXPJKWOQ, 2020.

Beck, H. E., Pan, M., Miralles, D. G., Reichle, R. H., Dorigo, W. A., Hahn, S., Sheffield, J., Karthikeyan, L., Balsamo, G., Parinussa, R. M., van Dijk, A. I. J. M., Du, J., Kimball, J. S., Vergopolan, N. and Wood, E. F.: Evaluation of 18 satellite- and model-based soil moisture products using in situ measurements from 826 sensors, Hydro. Earth Syst. Sci., 25, 17-40, https://doi.org/10.5194/hess-25-17-2021, 2021.

630 Bi, H., Ma, J., Zheng, W. and Zeng, J.: Comparison of soil moisture in GLDAS model simulations and in situ observations over the Tibetan Plateau, J. Geophys Res. Atmos., 121, 2658-2678, https://doi.org/10.1002/2015jd024131, 2016.

Bot, A. and Benites, J.: The importance of soil organic matter-key to drought-resistant soil and sustained food and production, FAO SOILS BULLETIN, Available at https://www.fao.org/3/a0100e/a0100e.pdf, 2005.

Brocca, L., Melone, F., Moramarco, T., Wagner, W. and Hasenauer, S.: ASCAT soil wetness index validation through in situ and modeled
635 soil moisture data in central Italy, Remote Sens. Environ., 114, 2745-2755, https://doi.org/10.1016/j.rse.2010.06.009, 2010.

Calvet, J.-C.: Investigating soil and atmospheric plant water stress using physiological and micrometeorological data, Agric. For. Meteorol., 103, 229-247, https://doi.org/10.1016/S0168-1923(00)00130-1, 2000.

Calvet, J.-C. and Noilhan, J.: From Near-Surface to Root-Zone Soil Moisture Using Year-Round Data, J. Hydrometeorol, 1, 393-400, https://doi.org/10.1175/1525-7541(2000)001<0393:FNSTRZ>2.0.CO;2, 2000.

640 CATDS: CATDS-PDC L4SM RZSM - 1 day global map of root zone soil moisture values from SMOS satellite, CATDS (CNES, IFREMER, CESBIO), http://dx.doi.org/10.12770/316e77af-cb72-4312-96a3-3011cc5068d4. Date Accessed 17-09-2021, 2021.

Cho, E., Choi, M. and Wagner, W.: An assessment of remotely sensed surface and root zone soil moisture through active and passive sensors in northeast Asia, Remote Sens. Environ., 160, 166-179, https://doi.org/10.1016/j.rse.2015.01.013, 2015.

CMA: Evaluation of Chinese ground-based air temperature grid dataset (V 2.0) (in Chinese), Accessed 6 April 2023, Available at
645 https://www.ckcest.cn/default/es3/detail/4004/dw_dataset/cccc30b0dcc368d608cd0c9db2dd5647, 2012a.

CMA: Evaluation of Chinese ground-based precipitation grid dataset (V 2.0) (in Chinese), Accessed 6 April 2023, Available at https://kgo.ckcest.cn/kgo/detail/4004/dw_dataset/4bd64984fde3209c6ce518e4f8de6caa.html, 2012b.

CMA: The Near-Real-Time Product Dataset Of The China Meteorological Administration Land Data Assimilation System (CLDAS-V2.0) Accessed 6 April 2023, AVailable at http://data.cma.cn/en/?r=search/uSearch&keywords=cldas, 2015.

650 Collow, T. W., Robock, A., Basara, J. B. and Illston, B. G.: Evaluation of SMOS retrievals of soil moisture over the central United States with currently available in situ observations, J. Geophys Res. Atmos., 117, D09113, https://doi.org/10.1029/2011jd017095, 2012.

Crow, W. T., Berg, A. A., Cosh, M. H., Loew, A., Mohanty, B. P., Panciera, R., de Rosnay, P., Ryu, D. and Walker, J. P.: Upscaling sparse ground-based soil moisture observations for the validation of coarse-resolution satellite soil moisture products, Rev. Geophys., 50, RG2002, https://doi.org/10.1029/2011rg000372, 2012.

https://doi.org/10.5194/egusphere-2023-1597
Preprint. Discussion started: 22 September 2023

Cui, H., Jiang, L., Du, J., Zhao, S., Wang, G., Lu, Z. and Wang, J.: Evaluation and analysis of AMSR-2, SMOS, and SMAP soil moisture products in the Genhe area of China, J. Geophys Res. Atmos., 122, 8650-8666, https://doi.org/10.1002/2017jd026800, 2017.

De Lannoy, G. J. M., Koster, R. D., Reichle, R. H., Mahanama, S. P. P. and Liu, Q.: An updated treatment of soil texture and associated hydraulic properties in a global land modeling system, J. Adv. Model Earth Syst., 6, 957-979, https://doi.org/10.1002/2014ms000330, 2014.

de Rosnay, P., Balsamo, G., Albergel, C., Muñoz-Sabater, J. and Isaksen, L.: Initialisation of Land Surface Variables for Numerical Weather Prediction, Surv. Geophys., 35, 607-621, https://doi.org/10.1007/s10712-012-9207-x, 2012.

Djamai, N., Magagi, R., Goïta, K., Hosseini, M., Cosh, M. H., Berg, A. and Toth, B.: Evaluation of SMOS soil moisture products over the CanEx-SM10 area, J. Hydrol., 520, 254-267, https://doi.org/10.1016/j.jhydrol.2014.11.026, 2015.

Douville, H., Viterbo, P., Mahfouf, J.-F. and Beljaars, A.: Evaluation of the optimum interpolation and nudging techniques for soil moisture analysis using FIFE data, Mon. Weather Rev., 128, 1733–1756, https://doi.org/10.1175/1520-0493(2000)128<1733:EOTOIA>2.0.CO;2, 2000.

Fan, L., Xing, Z., Lannoy, G. D., Frappart, F., Peng, J., Zeng, J., Li, X., Yang, K., Zhao, T., Shi, J., Ma, H., Wang, M., Liu, X., Yi, C., Ma, M., Tang, X., Wen, J., Chen, X., Wang, C., Wang, L., Wang, G. and Wigneron, J.-P.: Evaluation of satellite and reanalysis estimates of surface and root-zone soil moisture in croplands of Jiangsu Province, China, Remote Sens. Environ., 282, 113283, https://doi.org/10.1016/j.rse.2022.113283, 2022.

Fan, Y., Miguez-Macho, G., Jobbagy, E. G., Jackson, R. B. and Otero-Casal, C.: Hydrologic regulation of plant rooting depth, Proc. Natl. Acad. Sci. U. S. A., 114, 10572-10577, https://doi.org/10.1073/pnas.1712381114, 2017.

FAO, IIASA, ISRIC, ISSCAS and JRC: Harmonized World Soil Database (version 1.2), Feb 2012, Available at http://webarchive.iiasa.ac.at/Research/LUC/External-World-soil-database/HWSD_Documentation.pdf, 2012.

Fernandez-Moran, R., Wigneron, J. P., De Lannoy, G., Lopez-Baeza, E., Parrens, M., Mialon, A., Mahmoodi, A., Al-Yaari, A., Bircher, S., Al Bitar, A., Richaume, P. and Kerr, Y.: A new calibration of the effective scattering albedo and soil roughness parameters in the SMOS SM retrieval algorithm, Int. J. Appl. Earth Obs., 62, 27-38, https://doi.org/10.1016/j.jag.2017.05.013, 2017.

Ford, T. W., Harris, E. and Quiring, S. M.: Estimating root zone soil moisture using near-surface observations from SMOS, Hydrol. Earth Syst. Sci., 18, 139-154, https://doi.org/10.5194/hess-18-139-2014, 2014.

Gao, H., Birkel, C., Hrachowitz, M., Tetzlaff, D., Soulsby, C. and Savenije, H. H. G.: A simple topography-driven and calibration-free runoff generation module, Hydrol. Earth Syst. Sci., 23, 787-809, https://doi.org/10.5194/hess-23-787-2019, 2019.

Gao, H., Hrachowitz, M., Schymanski, S. J., Fenicia, F., Sriwongsitanon, N. and Savenije, H. H. G.: Climate controls how ecosystems size the root zone storage capacity at catchment scale, Geophys. Res. Lett., 41, 7916-7923, https://doi.org/10.1002/2014gl061668, 2014.

Gelaro, R., McCarty, W., Suarez, M. J., Todling, R., Molod, A., Takacs, L., Randles, C., Darmenov, A., Bosilovich, M. G., Reichle, R., Wargan, K., Coy, L., Cullather, R., Draper, C., Akella, S., Buchard, V., Conaty, A., da Silva, A., Gu, W., Kim, G. K., Koster, R., Lucchesi, R., Merkova, D., Nielsen, J. E., Partyka, G., Pawson, S., Putman, W., Rienecker, M., Schubert, S. D., Sienkiewicz, M. and Zhao, B.: The Modern-Era Retrospective Analysis for Research and Applications, Version 2 (MERRA-2), J. Clim., 30, 5419-5454, https://doi.org/10.1175/JCLI-D-16-0758.1, 2017.

Girotto, M., De Lannoy, G. J. M., Reichle, R. H. and Rodell, M.: Assimilation of gridded terrestrial water storage observations from GRACE into a land surface model, Water Resour. Res., 52, 4164-4183, https://doi.org/10.1002/2015wr018417, 2016.

GMAO: inst3_3d_asm_Cp: MERRA-2 3D IAU State, Meteorology Instantaneous 3-hourly (p-coord, 0.625x0.5L42), version 5.12.4, Greenbelt, MD, USA: Goddard Space Flight Center Distributed Active Archive Center (GSFC DAAC), Accessed 16 OCTOBER 2021, at doi: https://doi.org/10.5067/VJAFPLI1CSIV, 2015.

Gou, Q., Zhu, Y., Lü, H., Horton, R., Yu, X., Zhang, H., Wang, X., Su, J., Liu, E., Ding, Z., Wang, Z. and Yuan, F.: Application of an improved spatio-temporal identification method of flash droughts, J. Hydro., 604, 127224, https://doi.org/10.1016/j.jhydrol.2021.127224, 2022.

Gu, F., Chen, X., Wei, C., Zhou, M. and Li, B.: Distribution of calcareous concretion in soil profile and their effects on soil water retention in calcic vertisol (in Chinese with English abstract) , Transactions of the Chinese Society of Agricultural Engineering, 37, 73-80, https://doi.org/10.11975/j.issn.1002-6819.2021.06.010, 2021.

Hauser, M., Orth, R. and Seneviratne, S. I.: Role of soil moisture versus recent climate change for the 2010 heat wave in western Russia, Geophys. Res. Lett., 43, 2819-2826, https://doi.org/10.1002/2016gl068036, 2016.

Hersbach, H., Bell, B., Berrisford, P., Biavati, G., Horányi, A., Muñoz Sabater, J., Nicolas, J., Peubey, C., Radu, R., Rozum, I., Schepers, D., Simmons, A., Soci, C., Dee, D., and Thépaut, J.-N.: ERA5 hourly data on single levels from 1940 to present, Copernicus Climate

https://doi.org/10.5194/egusphere-2023-1597
Preprint. Discussion started: 22 September 2023

Change Service (C3S) Climate Data Store (CDS), https://doi.org/10.24381/cds.adbb2d47 (Accessed on 22 September 2021), 2023.

Hersbach, H., Bell, B., Berrisford, P., Hirahara, S., Horányi, A., Muñoz‐Sabater, J., Nicolas, J., Peubey, C., Radu, R., Schepers, D., Simmons, A., Soci, C., Abdalla, S., Abellan, X., Balsamo, G., Bechtold, P., Biavati, G., Bidlot, J., Bonavita, M., Chiara, G., Dahlgren, P., Dee, D., Diamantakis, M., Dragani, R., Flemming, J., Forbes, R., Fuentes, M., Geer, A., Haimberger, L., Healy, S., Hogan, R. J., Hólm, E., Janisková, M., Keeley, S., Laloyaux, P., Lopez, P., Lupu, C., Radnoti, G., Rosnay, P., Rozum, I., Vamborg, F., Villaume, S. and Thépaut, J. N.: The ERA5 global reanalysis, Q. J. R. Meteorol. Soc., 146, 1999-2049, https://doi.org/10.1002/qj.3803, 2020.

Houborg, R., Rodell, M., Li, B., Reichle, R. and Zaitchik, B. F.: Drought indicators based on model-assimilated Gravity Recovery and Climate Experiment (GRACE) terrestrial water storage observations, Water Resour. Res., 48, W07525, https://doi.org/10.1029/2011wr011291, 2012.

Huerta-Bátiz, H. E., Constantino-Recillas, D. E., Monsiváis-Huertero, A., Hernández-Sánchez, J. C., Judge, J. and Aparicio-García, R. S.: Understanding root-zone soil moisture in agricultural regions of Central Mexico using the ensemble Kalman filter, satellite-derived information, and the THEXMEX-18 dataset, International Journal of Digital Earth, 15, 52-78, https://doi.org/10.1080/17538947.2021.2012534, 2022.

Jiao, D., Xu, N., Yang, F. and Xu, K.: Evaluation of spatial-temporal variation performance of ERA5 precipitation data in China, Sci. Rep., 11, 17956, https://doi,org/10.1038/s41598-021-97432-y, 2021.

Kerr, Y. H., Waldteufel, P., Richaume, P., Wigneron, J. P., Ferrazzoli, P., Mahmoodi, A., Al Bitar, A., Cabot, F., Gruhier, C., Juglea, S. E., Leroux, D., Mialon, A. and Delwart, S.: The SMOS Soil Moisture Retrieval Algorithm, IEEE Trans. Geosci. Remote Sens., 50, 1384-1403, https://doi.org/10.1109/tgrs.2012.2184548, 2012.

Kerr, Y. H., Waldteufel, P., Wigneron, J. P., Martinuzzi, J. M., Font, J. and Berger, M.: Soil Moisture Retrieval from Space: The Soil Moisture and Ocean Salinity (SMOS) Mission, IEEE Trans. Geosci. Remote Sens., 39, 1729-1735, https://doi.org/10.1109/36.942551, 2001.

Kleidon, A.: Beyond Gaia: Thermodynamics of Life and Earth System Functioning., Clim. Change, 66, 271-319, https://doi.org/10.1023/B:CLIM.0000044616.34867.ec, 2014.

Koster, R. D., Suarez, M. J., Ducharne, A., Stieglitz, M. and Kumar, P.: A catchment-based approach to modeling land surface processes in a general circulation model: 1. Model structure, J. Geophys Res. Atmos., 105, 24809-24822, https://doi.org/10.1029/2000jd900327, 2000.

Li, B., Beaudoing, H., Rodell, M. and NASA/GSFC/HSL: GLDAS Catchment Land Surface Model L4 daily 0.25 x 0.25 degree GRACE-DA1 V2.2, Greenbelt, Maryland, USA, Goddard Earth Sciences Data and Information Services Center (GES DISC), Accessed: [Data Access Date], https://doi.org/10.5067/TXBMLX370XX8, 2020.

Li, B., Rodell, M., Kumar, S., Beaudoing, H. K., Getirana, A., Zaitchik, B. F., Goncalves, L. G., Cossetin, C., Bhanja, S., Mukherjee, A., Tian, S., Tangdamrongsub, N., Long, D., Nanteza, J., Lee, J., Policelli, F., Goni, I. B., Daira, D., Bila, M., Lannoy, G., Mocko, D., Steele‐Dunne, S. C., Save, H. and Bettadpur, S.: Global GRACE Data Assimilation for Groundwater and Drought Monitoring: Advances and Challenges, Water Resour. Res., 55, 7564-7586, https://doi.org/10.1029/2018wr024618, 2019.

Li, B., Rodell, M., Zaitchik, B. F., Reichle, R. H., Koster, R. D. and van Dam, T. M.: Assimilation of GRACE terrestrial water storage into a land surface model: Evaluation and potential value for drought monitoring in western and central Europe, J. Hydrol., 446-447, 103-115, https://doi.org/10.1016/j.jhydrol.2012.04.035, 2012.

Li, D., Zhang, g. and Gong, z.: On Taxonomy of Shajiang Black Soils in China (in Chinese with English abstract), Soils, 43, 623-629, https://doi.org/10.13758/j.cnki.tr.2011.04.015, 2011.

Li, X., Wigneron, J.-P., Frappart, F., Fan, L., Ciais, P., Fensholt, R., Entekhabi, D., Brandt, M., Konings, A. G., Liu, X., Wang, M., Al-Yaari, A. and Moisy, C.: Global-scale assessment and inter-comparison of recently developed/reprocessed microwave satellite vegetation optical depth products, Remote Sens. Environ., 253, 112208, https://doi.org/10.1016/j.rse.2020.112208, 2021.

Ling, X., Huang, Y., Guo, W., Wang, Y., Chen, C., Qiu, B., Ge, J., Qin, K., Xue, Y. and Peng, J.: Comprehensive evaluation of satellite-based and reanalysis soil moisture products using in situ observations over China, Hydrol. Earth Syst. Sci., 25, 4209-4229, https://doi.org/10.5194/hess-25-4209-2021, 2021.

Liu, E., Zhu, Y., Lü, H., Horton, R., Gou, Q., Wang, X., Ding, Z., Xu, H. and Pan, Y.: Estimation and Assessment of the Root Zone Soil Moisture from Near-Surface Measurements over Huai River Basin, Atmosphere, 14, 124-145, https://doi.org/10.3390/atmos14010124, 2023.

Lorenz, R., Jaeger, E. B. and Seneviratne, S. I.: Persistence of heat waves and its link to soil moisture memory, Geophys. Res. Lett., 37, L09703, https://doi.org/10.1029/2010gl042764, 2010.

https://doi.org/10.5194/egusphere-2023-1597
Preprint. Discussion started: 22 September 2023

Ma, H., Zeng, J., Chen, N., Zhang, X., Cosh, M. H. and Wang, W.: Satellite surface soil moisture from SMAP, SMOS, AMSR2 and ESA CCI: A comprehensive assessment using global ground-based observations, Remote Sens. Environ., 231, 111215, https://doi.org/10.1016/j.rse.2019.111215, 2019.

McCarty, W., Coy, L., Gelaro, R., Huang, A., Merkova, D., Smith, E. B., Sienkiewicz, M. and Wargan, K.: MERRA-2 Input Observations: Summary and Assessment NASA Tech. Rep. Series on Global Modeling and Data Assimilation 46, 1-64, https://gmao.gsfc.nasa.gov/pubs/docs/McCarty885.pdf, 2016.

MWR: Specifications for soil moisture monitoring (in chinese), Available at http://www.jsgg.com.cn/Index/Display.asp?NewsID=21094., 2015.

Nachtergaele, F., Velthuizen, H. v., LucVerelst, Batjes, N., Dijkshoorn, K., Engelen, V. v., Fischer, G., Jones, A., Montanarella, L., Petri, M., Prieler, S., Xuezheng, S. and Teixeira, E. a. W., D.: The harmonized world soil database, 2010 19th World Congress of Soil Science, Soil Solutions for a Changing World, Aavilable at https://www.researchgate.net/profile/Niels-Batjes/publication/259975239_The_harmonized_world_soil_database/links/0deec52ed08ea33a81000000/The-harmonized-world-soil-database.pdf, 2009.

Pablos, M., González-Zamora, Á., Sánchez, N. and Martínez-Fernández, J.: Assessment of Root Zone Soil Moisture Estimations from SMAP, SMOS and MODIS Observations, Remote Sens., 10, 981, https://doi.org/10.3390/rs10070981, 2018.

Piani, C., Weedon, G. P., Best, M., Gomes, S. M., Viterbo, P., Hagemann, S. and Haerter, J. O.: Statistical bias correction of global simulated daily precipitation and temperature for the application of hydrological models, J. Hydrol., 395, 199-215, https://doi,org/10.1016/j.jhydrol.2010.10.024, 2010.

Qin, Y., Wu, T., Wu, X., Li, R., Xie, C., Qiao, Y., Hu, G., Zhu, X., Wang, W. and Shang, W.: Assessment of reanalysis soil moisture products in the permafrost regions of the central of the Qinghai-Tibet Plateau, Hydrol. Process., 31, 4647-4659, https://doi.org/10.1002/hyp.11383, 2017.

Rao, K. S., Chandra, G. and Rao, P. V. N.: The relationship between brightness temperature and soil moisture Selection of frequency range for microwave remote sensing, Int. J. Remote Sens., 8, 1531-1545, https://doi.org/10.1080/01431168708954795, 2007.

Reichle, R., Crow, W., Koster, R., Kimball, J. and Lannoy, G. D.: Algorithm Theoretical Basis Document (ATBD) SMAP Level 4 Surface and Root Zone Soil Moisture (L4_SM) Data Product, Soil Moisture Active Passive (SMAP) Project, Available at https://smap.jpl.nasa.gov/files/smap2/L4_SM_InitRel_v1.pdf, 2012.

Reichle, R., G. De Lannoy, R. D. Koster, W. T. Crow, J. S. Kimball and Liu, Q.: SMAP L4 Global 3-hourly 9 km EASE-Grid Surface and Root Zone Soil Moisture Geophysical Data, Version 5 [Data Set], Boulder, Colorado USA. NASA National Snow and Ice Data Center Distributed Active Archive Center, https://doi.org/10.5067/9LNYIYOBNBR5. Date Accessed 06-04-2021, 2020.

Reichle, R. H., De Lannoy, M., G. J. and Liu, Q.: Assessment of the SMAP Level-4 Surface and Root-Zone Soil Moisture Product Using In Situ Measurements, J. Hydrometeorol., 18, 2621-2645, https://doi.org/10.1175/jhm-d-17-0063.1, 2017a.

Reichle, R. H., De Lannoy, G. J. M., Liu, Q., Koster, R. D., Kimball, J. S., Crow, W. T., Ardizzone, J. V., Chakraborty, P., Collins, D. W., Conaty, A. L., Girotto, M., Jones, L. A., Kolassa, J., Lievens, H., Lucchesi, R. A. and Smith, E. B.: Global Assessment of the SMAP Level-4 Surface and Root-Zone Soil Moisture Product Using Assimilation Diagnostics, J. Hydrometeorol., 18, 3217-3237, https://doi.org/10.1175/JHM-D-17-0130.1, 2017b.

Reichle, R. H., Joseph V. Ardizzone, Gi-Kong Kim, Robert A. Lucchesi, Edmond B. Smith and Weiss, a. B. H.: Soil Moisture Active Passive (SMAP) Mission Level 4 Surface and Root Zone Soil Moisture (L4_SM) Product Specification Document, GMAO Office Note No. 10 (Version 1.4), 82 pp, NASA Goddard Space Flight Center, Greenbelt, MD, USA., Available from http://gmao.gsfc.nasa.gov/pubs/office_notes, 2015.

Reichle, R. H., Liu, Q., Koster, R. D., Ardizzone, J. V., Colliander, A., Crow, W. T., De Lannoy, G. J. M. and Kimball, J. S.: Soil Moisture Active Passive (SMAP) Project Assessment Report for Version 5 of the L4_SM Data Product, Technical Report Series on Global Modeling and Data Assimilation, Volume 58, Available at https://ntrs.nasa.gov/api/citations/20210018731/downloads/TM-2021-104606%20Vol.%2058%20SMAP_L4_SM_Version_5_Release_Assessment_Report_final-v.3.pdf, 2021.

Reichle, R. H., Liu, Q., Koster, R. D., Draper, C. S., Mahanama, S. P. P. and Partyka, G. S.: Land Surface Precipitation in MERRA-2, J. Clim., 30, 1643-1664, https://doi.org/10.1175/jcli-d-16-0570.1, 2017c.

Reynolds, C. A., Jackson, T. J. and Rawls, W. J.: Estimating soil water-holding capacities by linking the Food and Agriculture Organization Soil map of the world with global pedon databases and continuous pedotransfer functions, Water Resour. Res., 36, 3653-3662, https://doi.org/10.1029/2000wr900130, 2000.

https://doi.org/10.5194/egusphere-2023-1597
Preprint. Discussion started: 22 September 2023

Rienecker, M. M., Suarez, M. J., Todling, R., Bacmeister, J., Takacs, L., Liu, H.-C., Gu, W., Sienkiewicz, M., Koster, R. D., Gelaro, R., Stajner, I. and Nielsen, J. E.: The GEOS-5 Data Assimilation System—Documentation of Versions 5.0.1, 5.1.0, and 5.2.0 NASA Tech. Rep. Series on Global Modeling and Data Assimilation, Available at https://ntrs.nasa.gov/api/citations/20120011955/downloads/20120011955.pdf, 2008.

Rodell, M., Houser, P. R., Jambor, U., Gottschalck, J., Mitchell, K., Meng, C. J., Arsenault, K., Cosgrove, B., Radakovich, J., Bosilovich, M., Entin, J. K., Walker, J. P., Lohmann, D. and Toll, D.: The Global Land Data Assimilation System, B. Am. Meteorol. Soc., 85, 381-394, https://doi.org/10.1175/bams-85-3-381, 2004.

Rui, H., Beaudoing, H. and Loeser, C.: README Document for NASA GLDAS Version 2 Data Products, Available at https://hydro1.gesdisc.eosdis.nasa.gov/data/GLDAS/GLDAS_NOAH025_3H.2.1/doc/README_GLDAS2.pdf, 2021.

Saha, S. and coauthors: updated daily. NCEP Climate Forecast System Version 2 (CFSv2) 6-hourly Products, Research Data Archive at the National Center for Atmospheric Research, Computational and Information Systems Laboratory, https://doi.org/10.5065/D61C1TXF. Accessed 28 October 2021, 2011.

Saha, S., Moorthi, S., Pan, H.-L., Wu, X., Wang, J., Nadiga, S., Tripp, P., Kistler, R., Woollen, J., Behringer, D., Liu, H., Stokes, D., Grumbine, R., Gayno, G., Wang, J., Hou, Y.-T., Chuang, H.-y., Juang, H.-M. H., Sela, J., Iredell, M., Treadon, R., Kleist, D., Van Delst, P., Keyser, D., Derber, J., Ek, M., Meng, J., Wei, H., Yang, R., Lord, S., van den Dool, H., Kumar, A., Wang, W., Long, C., Chelliah, M., Xue, Y., Huang, B., Schemm, J.-K., Ebisuzaki, W., Lin, R., Xie, P., Chen, M., Zhou, S., Higgins, W., Zou, C.-Z., Liu, Q., Chen, Y., Han, Y., Cucurull, L., Reynolds, R. W., Rutledge, G. and Goldberg, M.: The NCEP Climate Forecast System Reanalysis, B. Am. Meteorol. Soc., 91, 1015-1058, https://doi.org/10.1175/2010bams3001.1, 2010.

Saha, S., Moorthi, S., Wu, X., Wang, J., Nadiga, S., Tripp, P., D., B., Hou, Y., Chuang, H. and Iredell, M.: The NCEP Climate Forecast System Version 2, J. Clim., 27, 2185-2208, https://doi.org/10.1175/JCLI-D-12-00823.1, 2014.

Seuffert, G., Wilker, H., Viterbo, P., Mahfouf, J. F., Drusch, M. and Calvet, J. C.: Soil moisture analysis combining screen-level parameters and microwave brightness temperature: A test with field data, Geophys. Res. Lett., 30, https://doi.org/10.1029/2003gl017128, 2003.

Shangguan, W., Dai, Y., Liu, B., Zhu, A., Duan, Q., Wu, L., Ji, D., Ye, A., Yuan, H., Zhang, Q., Chen, D., Chen, M., Chu, J., Dou, Y., Guo, J., Li, H., Li, J., Liang, L., Liang, X., Liu, H., Liu, S., Miao, C. and Zhang, Y.: A China data set of soil properties for land surface modeling, J. Adv. Model. Earth Syst., 5, 212-224, https://doi.org/10.1002/jame.20026, 2013.

Shi, C., Jiang, L., Zhang, T., Xu, B. and Han, S.: Status and Plans of CMA Land Data Assimilation System (CLDAS) Project, Geophys. Res. Lett., 16, EGU2014-5671, Available at https://meetingorganizer.copernicus.org/EGU2014/EGU2014-5671.pdf, 2014.

Su, J., Lü, H., Zhu, Y., Cui, Y. and Wang, X.: Evaluating the hydrological utility of latest IMERG products over the Upper Huaihe River Basin, China, Atmos. Res., 225, 17-29, https://doi.org/10.1016/j.atmosres.2019.03.025, 2019.

Sun, Y., Solomon, S., Dai, A. and W. Portmann, R.: How Often Does It Rain?, J. Clim., 19, 916-934, https://doi.org/10.1175/JCLI3672.1, 2005.

Tangdamrongsub, N., Han, S.-C., Yeo, I.-Y., Dong, J., Steele-Dunne, S. C., Willgoose, G. and Walker, J. P.: Multivariate data assimilation of GRACE, SMOS, SMAP measurements for improved regional soil moisture and groundwater storage estimates, Adv. Water Resour., 135, 103477, https://doi.org/10.1016/j.advwatres.2019.103477, 2020.

Tian, S., Tregoning, P., Renzullo, L. J., van Dijk, A. I. J. M., Walker, J. P., Pauwels, V. R. N. and Allgeyer, S.: Improved water balance component estimates through joint assimilation of GRACE water storage and SMOS soil moisture retrievals, Water Resour. Res., 53, 1820-1840, https://doi.org/10.1002/2016wr019641, 2017.

Velasquez, P., Messmer, M. and Raible, C. C.: A new bias-correction method for precipitation over complex terrain suitable for different climate states: a case study using WRF (version 3.8.1), Geosci. Model Dev., 13, 5007-5027, https://doi,org/10.5194/gmd-13-5007-2020, 2020.

Wang, A. and Zeng, X.: Evaluation of multireanalysis products with in situ observations over the Tibetan Plateau, J. Geophys Res., 117, D05102, https://doi.org/10.1029/2011JD016553, 2012.

Wang, X., Lü, H., Crow, W. T., Zhu, Y., Wang, Q., Su, J., Zheng, J. and Gou, Q.: Assessment of SMOS and SMAP soil moisture products against new estimates combining physical model, a statistical model, and in-situ observations: A case study over the Huai River Basin, China, J. Hydro., 598, 126468, https://doi.org/10.1016/j.jhydrol.2021.126468, 2021a.

Wang, Z., Che, T., Zhao, T., Dai, L., Li, X. and Wigneron, J.-P.: Evaluation of SMAP, SMOS, and AMSR2 Soil Moisture Products Based on Distributed Ground Observation Network in Cold and Arid Regions of China, IEEE J-STARS, 14, 8955-8970, https://doi.org/10.1109/jstars.2021.3108432, 2021b.

https://doi.org/10.5194/egusphere-2023-1597
Preprint. Discussion started: 22 September 2023

Wigneron, J.-P., Li, X., Frappart, F., Fan, L., Al-Yaari, A., De Lannoy, G., Liu, X., Wang, M., Le Masson, E. and Moisy, C.: SMOS-IC data record of soil moisture and L-VOD: Historical development, applications and perspectives, Remote Sens. Environ., 254, 112238, https://doi.org/10.1016/j.rse.2020.112238, 2021.

Wösten, J. H. M., Pachepsky, Y. A. and Rawls, W. J.: Pedotransfer functions: Bridging the gap between available basic soil data and missing soil hydraulic characteristics, J. Hydrol., 251, 123-150, https://doi.org/10.1016/S0022-1694(01)00464-4, 2001.

Xia, Y., Sheffield, J., Ek, M. B., Dong, J., Chaney, N., Wei, H., Meng, J. and Wood, E. F.: Evaluation of multi-model simulated soil moisture in NLDAS-2, J. Hydrol., 512, 107-125, https://doi.org/10.1016/j.jhydrol.2014.02.027, 2014.

Xing, Z., Fan, L., Zhao, L., De Lannoy, G., Frappart, F., Peng, J., Li, X., Zeng, J., Al-Yaari, A., Yang, K., Zhao, T., Shi, J., Wang, M., Liu, X., Hu, G., Xiao, Y., Du, E., Li, R., Qiao, Y., Shi, J., Wen, J., Ma, M. and Wigneron, J.-P.: A first assessment of satellite and reanalysis estimates of surface and root-zone soil moisture over the permafrost region of Qinghai-Tibet Plateau, Remote Sens. Environ., 265, 112666, https://doi.org/10.1016/j.rse.2021.112666, 2021.

Xu, L., Chen, N., Zhang, X., Moradkhani, H., Zhang, C. and Hu, C.: In-situ and triple-collocation based evaluations of eight global root zone soil moisture products, Remote Sens. Environ., 254, 112248, https://doi.org/10.1016/j.rse.2020.112248, 2021.

Yang, S., Li, R., Wu, T., Hu, G., Xiao, Y., Du, Y., Zhu, X., Ni, J., Ma, J., Zhang, Y., Shi, J. and Qiao, Y.: Evaluation of reanalysis soil temperature and soil moisture products in permafrost regions on the Qinghai-Tibetan Plateau, Geoderma, 377, 114583, https://doi.org/10.1016/j.geoderma.2020.114583, 2020.

Yang, Y., Donohue, R. J. and McVicar, T. R.: Global estimation of effective plant rooting depth: Implications for hydrological modeling, Water Resour. Res., 52, 8260-8276, https://doi.org/10.1002/2016wr019392, 2016.

Zaitchik, B. F., Rodell, M. and Reichle, R. H.: Assimilation of GRACE Terrestrial Water Storage Data into a Land Surface Model: Results for the Mississippi River Basin, J. Hydrometeorol., 9, 535-548, https://doi.org/10.1175/2007jhm951.1, 2008.

Zeng, J., Yuan, X., Ji, P. and Shi, C.: Effects of meteorological forcings and land surface model on soil moisture simulation over China, J. Hydrol., 603, 126978, https://doi.org/10.1016/j.jhydrol.2021.126978, 2021.

Zha, L., Wu, K., Li, L., Chen, J. and Ju, B.: The Cultivation Obstacle Factors of Lime Concretion Black Soil Genuses in Henan (in Chinese with English abstract) , Chinese Journal of Soil Science, 46, 280-286, https://doi.org/10.19336/j.cnki.trtb.2015.02.004, 2015.

Zhang, Y., Wang, Y. and Liu, L.: Function Mechanism Between the Drought and Waterlogging Disaster and the Soil - structure of the Shajiang Soil in Huaibei Plain, Prog. Gengr., 20, 169-176, https://doi.org/10.11820/dlkxjz.2001.02.010, 2001.

Zhang, Y., Xia, J., Liang, T. and Shao, Q.: Impact of Water Projects on River Flow Regimes and Water Quality in Huai River Basin, Water Resour. Manag., 24, 889-908, https://doi.org/10.1007/s11269-009-9477-3, 2009.

Zheng, J., Zhao, T., Lü, H., Shi, J., Cosh, M. H., Ji, D., Jiang, L., Cui, Q., Lu, H., Yang, K., Wigneron, J.-P., Li, X., Zhu, Y., Hu, L., Peng, Z., Zeng, Y., Wang, X. and Kang, C. S.: Assessment of 24 soil moisture datasets using a new in situ network in the Shandian River Basin of China, Remote Sens. Environ., 271, 112891, https://doi.org/10.1016/j.rse.2022.112891, 2022.

Zhou, J., Wu, Z., Crow, W. T., Dong, J. and He, H.: Improving Spatial Patterns Prior to Land Surface Data Assimilation via Model Calibration Using SMAP Surface Soil Moisture Data, Water Resour. Res., 56, e2020WR027770, https://doi.org/10.1029/2020wr027770, 2020.